University of Nebraska - Lincoln

DigitalCommons@University of Nebraska - Lincoln

3-30-2001

Modeling a spring wheat crop under elevated CO_2 and drought

S. Grossman-Clarke
Arizona State University

P. J. Pinter Jr.
Potsdam Institute for Climate Impact Research, 14412 Potsdam, Germany

T. Kartschall
USDA-ARS, US Water Conservation Laboratory, Phoenix, Arizona

B. A. Kimball
Potsdam Institute for Climate Impact Research, 14412 Potsdam, Germany, bruce.kimball@ars.usda.gov

D. J. Hunsaker
Potsdam Institute for Climate Impact Research, 14412 Potsdam, Germany, doug.hunsaker@usda.gov

See next page for additional authors

Grossman-Clarke, S.; Pinter, P. J. Jr.; Kartschall, T.; Kimball, B. A.; Hunsaker, D. J.; Wall, G. W.; Garcia, R. L.; and LaMorte, R. L., "Modeling a spring wheat crop under elevated CO_2 and drought" (2001). *Publications from USDA-ARS / UNL Faculty*. 209.
https://digitalcommons.unl.edu/usdaarsfacpub/209

Authors

S. Grossman-Clarke, P. J. Pinter Jr., T. Kartschall, B. A. Kimball, D. J. Hunsaker, G. W. Wall, R. L. Garcia, and R. L. LaMorte

Modelling a spring wheat crop under elevated CO_2 and drought

S. Grossman-Clarke[1], P. J. Pinter Jr[2], T. Kartschall[3], B. A. Kimball[2], D. J. Hunsaker[2], G. W. Wall[2], R. L. Garcia[4] and R. L. LaMorte[2]

[1]Arizona State University, Environmental Fluid Dynamics Program, PO Box 879809, Tempe, Arizona 85287–9809, USA; [2]Potsdam Institute for Climate Impact Research, PO Box 60 12 03, 14412 Potsdam, Germany; [3]USDA, Agricultural Research Service, US Water Conservation Laboratory, Phoenix, Arizona, 85040, USA; [4]LI-COR Inc., 4221 Superior Street, Lincoln, Nebraska 68504, USA

Summary

Author for correspondence:
Susanne Grossman-Clarke
Tel: +1 480 727 6660
Fax: +1 480 965 8746
Email: sg.clarke.asu.edu

• The simulation model DEMETER was used here to investigate which mechanisms led to a larger CO_2 effect on biomass production and yield of a spring wheat crop under drought compared with unlimited water supply.
• Field data of the free-air CO_2 enrichment (FACE) wheat experiments in Arizona (1993–94) were used to test the model. The influence of a particular mechanism leading to a higher CO_2 effect under drought was investigated by eliminating the influence of the other causes on the simulation results on selected days during the growing seasons.
• A larger CO_2 effect under drought was caused in the model by the lower potential transpiration rate, higher root biomass and the nonlinear functional dependence of net assimilation rate on leaf internal CO_2 concentration. The contribution of the different mechanisms changed in significance during the growing season depending on the degree of soil water limitation. The model successfully described the qualitative and quantitative behaviour of the crop under elevated CO_2.
• A well-tested simulation model can be a useful tool in understanding the complex interactions underlying observed ecosystem responses to stress under elevated CO_2.

Key words: elevated CO_2, spring wheat, simulation model, soil water limitation, CO_2 effect.

© *New Phytologist* (2001) **150**: 315–335

Introduction

Numerous experimental studies have been conducted to investigate the effect of elevated atmospheric CO_2 concentrations on economically important agricultural crops. The results for grain crops with the C_3 photosynthesis mechanism revealed an average increase in growth and yield of about 30% for a doubling of the recent atmospheric CO_2 concentration (reviews in Kimball & Idso, 1983; Kimball, 1983; Cure & Acock, 1986; Kimball *et al.*, 1995; Pinter *et al.*, 1996). For crops grown under field conditions, the positive impact of elevated atmospheric CO_2 concentrations on productivity was found to be significantly stronger under soil water limitation than under potential growth conditions, as reported in Kimball *et al.* (1994) for cotton, Pinter *et al.* (1996) for wheat, De Luis *et al.* (1999) for alfalfa and also for temperate pasture species (Clark *et al.*, 1999). A series of mechanisms moderating the effect of drought on

plant productivity under elevated atmospheric CO_2 concentrations is conceivable (Amthor, 1999; Hsiao & Jackson, 1999): (1) The rate of potential transpiration (i.e. transpiration under unlimited soil water supply) on a leaf area basis is lower under elevated atmospheric CO_2 concentrations due to CO_2-induced stomatal closure (Morison, 1998). Depending on the biomass increase, the potential transpiration at the canopy level might also be lower under elevated CO_2. Under these circumstances, the degree to which the potential assimilation rate is fulfilled under water limitation is higher under elevated than under ambient CO_2 concentrations. Furthermore, soil water depletion in the root zone might occur at a slower rate than for plants growing under ambient CO_2 concentrations; (2) In the long term it is possible that the higher root biomass leads to higher water availability for the crop grown under elevated CO_2; (3) We suggest that elevated CO_2 weakens 'stomatal' effects of water limitation on leaf net assimilation rate (A_n) that is the

reduction of the leaf internal CO_2 concentration (c_i) under short-term drought by stomatal closure and a preference of oxygenation relative to carboxylation (Daley *et al.*, 1989; Stitt, 1991; Therashima, 1992; Cornic, 1994). The higher slope of the A_n-c_i curve for lower CO_2 concentrations leads to a stronger reduction of A_n under ambient than under elevated CO_2.

Mechanisms (1) and (2) improve the plant water status leading to a higher leaf water potential (Ψ_l) under elevated CO_2 and therefore higher rates of leaf extension and leaf growth (Huber *et al.*, 1984; Allen *et al.*, 1994; Grant *et al.*, 1999). 'Nonstomatal' effects of drought on photosynthesis might be reduced under elevated CO_2 by alleviating the reduction in c_i. A decrease in c_i due to drought-induced stomatal closure is assumed to initiate 'nonstomatal' effects on photosynthesis (Hsiao and Jackson, 1999). Other possible interactions between drought and elevated CO_2 resulting from an improved water status are related to changes in canopy temperature, respiration and senescence rate.

A comprehensive data set is available from the free-air carbon dioxide enrichment (FACE) wheat experiments in Arizona (1993–1994), where spring wheat was grown under CO_2 mole fractions of 360 μmol mol^{-1} and 550 μmol mol^{-1} and subjected to two water treatments, sufficient and limited water supply. The results have been published (Kimball *et al.*, 1995; Pinter *et al.*, 1996; Wechsung *et al.*, 1999). These show that the average CO_2 effect of the two experiments (expressed as the percent change of the value obtained at ambient atmospheric CO_2 concentration) on mid-season canopy assimilation rate, aboveground green biomass and yield was higher under soil water limitation than under potential growth conditions by 25%, 4% and 12%, respectively. The CO_2 effect on water use efficiency, based on the ratio of grain yield to the seasonal sum of the crop water use, was 7% higher under soil water limitation (Hunsaker *et al.*, 1996).

The objective of this paper is to investigate how different mechanisms contributed to the higher CO_2 effect, under soil water limitation, for this spring wheat crop, using the wheat growth model DEMETER (Kartschall *et al.*, 1996). First, numerical results for primary production, yield and water use were compared with the field data to test the capacity of the model to describe the higher impact of the elevated CO_2 concentration under limited compared with unlimited soil water supply. The influence of a particular mechanism leading to this result was then investigated by eliminating the influence of other causes and analysing to what degree this changed the simulation results on selected days during the growing seasons.

DEMETER contains a model integrating energy balance, photosynthesis and stomatal conductance (g_s) (Grossman-Clarke *et al.*, 1999), which allows it to simulate the reduced potential transpiration under elevated CO_2 and 'stomatal' effects of soil water depletion on photosynthesis due to changes in c_i. However, the leaf water potential was not explicitly described in DEMETER, which is based on results of Tardieu & Simonneau (1998) who showed that stomatal conductance of anisohydric plants (plants with changing leaf water potential during a day) is independent of leaf water potential, but controlled by soil water limitation effects on the concentration of ABA in the xylem. Other studies also support the hypothesis that the effect of soil water limitation on stomata is mediated by chemical signals and not by plant water status (Schulze *et al.*, 1987; Davies & Zhang, 1991; Hartung & Slovik, 1991; Gollan *et al.*, 1992; Daeter & Hartung, 1995).

For describing the influence of the plant water status on growth and other physiological processes the crop water stress index $I_s = (1 - E_c/E_p)$, with E_c being canopy transpiration and E_p potential transpiration (Jackson *et al.*, 1981) was used. It was shown in different studies that I_s is strongly correlated with plant water potential (Ehrler *et al.*, 1978; Idso *et al.*, 1981; Pinter & Reginato, 1982). Long-term effects on root growth and the influence on the water availability of the crop under elevated CO_2 are simulated in DEMETER.

Simulation studies concerning the effect of elevated CO_2 on growth and water use of a spring wheat crop under soil water limitation were carried out by Tubiello *et al.* (1999) and Grant *et al.* (1999) using the CERES and *ecosys* models, respectively. Grant *et al.* (1999) assumed that the higher impact of elevated CO_2 under soil water limitation was a result of the higher leaf water potential under elevated CO_2. In *ecosys* this is assumed to cause a smaller reduction of stomatal conductance when leaf water potential is lowered by soil water depletion, leading to a greater rise in leaf net assimilation rate due to elevated CO_2 compared with the condition of unlimited soil water supply.

Materials and Methods

Field experiment

The FACE wheat experiment was conducted on a field at the Maricopa Agricultural Center of the University of Arizona, *c.* 50 km south of Phoenix in the midst of an extensive agricultural region (33.07° N latitude, 111.98° W longitude, 358-m altitude), to investigate the effects of elevated atmospheric CO_2 on field grown wheat (Kimball *et al.*, 1995; Hunsaker *et al.*, 1996; Pinter *et al.*, 1996). Spring wheat (*Triticum aestivum* L. cv. Yecora Rojo) was sown in December (1992 and 1993) and harvested in late May 1993 and June in 1994. FACE apparatus was used to enrich the air to about 550 μmol mol^{-1} in four 25 m diameter circular plots. Four replicate control rings at ambient CO_2 were also installed.

In the FACE plots, CO_2 enrichment began shortly after emergence, continuing until shortly before harvest and was in operation 24 h a day except for the last 2 wk of January 1993, when heavy rains prevented regular CO_2 delivery and enrichment was shortened to daylight hours to conserve supplies. During the experiment, it was possible to control CO_2 mole fraction in the FACE arrays to 550 μmol mol^{-1} $\pm$ 20% (Hendrey *et al.*, 1993).

Half of each plot was subjected to a drought treatment (DRY treatment). Plants grown with adequate water (WET treatment) were irrigated when the available water in the root zone was depleted to 70%. In 1993 plants grown under the DRY treatment were irrigated on the same day as those in the WET treatment, but received only 50% of the amount of water. During 1994, plants in the DRY treatment received the same amount as the plants in the WET treatment, but only on every other irrigation. The cumulative irrigation total between crop emergence and harvest was 603 mm for the WET treatment and 275 mm for the DRY treatment in 1993 and 599 mm and 257 mm in 1994, respectively. Cumulative rainfall during the same periods was 84 mm in 1993 and 65 mm in 1994. Irrigation water and fertilizer were delivered through a subsurface drip system. The wheat crop received 277 kg N ha^{-1} in 1993 and 261 kg N ha^{-1} in 1994.

Micrometeorological variables were recorded every minute using a data logging system (Campbell Scientific, Logan, UT, USA; Model CR7X). Diurnal changes in the sum of canopy transpiration and soil evaporation were determined as a residual in the energy balance (Kimball *et al.*, 1994), that is as the difference between net radiation of the canopy, soil heat flux and sensible heat flux. Net radiation was measured with duplicate net radiometers (Radiation Energy Balance System, Seattle, WA, USA; Model Q6) and soil heat flux was determined by soil heat flux plates (Radiation Energy Balance System; Model HFT-3). Sensible heat flux was determined by measuring the temperature difference between the crop surface and the air and then dividing the temperature difference by an aerodynamic resistance calculated from a measurement of wind speed (R. M. Young Co., Traverse City, MI, USA Model 12170C 3-cup anemometer with photochopper) at the 2-m height at one position in the field. The air temperature was measured at 2 m in each plot with an aspirated psychrometer. Crop surface temperature was measured with duplicate infrared thermometers (Everest Interscience, Fullerton, CA, USA; IRT Model 4000AL, 15° field of view) mounted above each plot to view the canopy toward the north at an angle of 20° below horizontal.

The daily and seasonal sums of canopy transpiration and soil evaporation were determined by measuring the change in soil water content over a period of time and calculating the soil water balance for those periods between soil water measurements where rainfall was small (less than 10 mm), irrigation water was not applied and where deep percolation could be reasonably assumed negligible, that is waiting at least 2 d after irrigation or heavy rainfall before taking the water content measurements. Volumetric soil water contents were measured in each plot using Time-Domain Reflectometry (TDR) and neutron scattering equipment. A 2-m-long neutron probe access tube was installed vertically in the plant row, 0.9 m from the TDR probe, and with the same placement as the TDR probe relative to the drip emitters. A neutron moisture gauge, calibrated at the field site, was used to measure volumetric soil water contents in 0.2-m intervals from 0.4 to 2.0 m. Water contents were measured about once every week from crop emergence through the first regular irrigation. After that, water contents were measured every 2 to 5 d depending on the frequency of irrigation.

Wheat plants were sampled at 7- to 10-d intervals during the two growing seasons. A minimum of six plants was obtained from four sampling zones in each subplot (24 plants total). Plant phenology, green biomass and green leaf area were determined from a subsample of 12 median-sized plants per plot. Dried biomass was determined for crown, stem, green leaf, nongreen leaf, and head components of all 24 plants after oven-drying at 65–70°C. Leaf area index was computed from the leaf mass per unit, green leaf area, green leaf biomass of all plants and plant density. Beginning 1 wk after anthesis, developing grains were separated from the chaff by a combination of hand and machine threshing of the heads and oven-dried for a total of 14 d at 65–70°C. Final grain yields were determined by machine harvest of *c.* 20 m^2 of each subplot.

Model description

The wheat model DEMETER includes submodels for the simulation of plant and root growth, soil carbon, nitrogen and temperature dynamics (Kartschall *et al.*, 1989), soil water dynamics and the integrated calculation of assimilation rate and energy fluxes between the plant canopy and the atmosphere (Grossman-Clarke *et al.*, 1999). The overall simulation time step is one hour. The sources for mathematical descriptions of essential growth processes and their parameterization for spring wheat follow: van Keulen & Seligman (1987): phenology; allocation pattern for assimilates and nitrogen to leaves, stems, roots and ears. Penning de Vries & van Laar (1982): growth respiration and biomass growth. Penning de Vries *et al.* (1989): maintenance respiration. Goudriaan & van Laar (1994): radiation balance for direct and diffuse radiation at different levels inside the canopy. Asseng (1989): root growth. Groot (1987): Water and nitrogen uptake from the soil. Kartschall *et al.* (1996): senescence rate and grain filling.

The volumetric soil water content depending on time and soil depth is determined by means of the numerical solution of the Richards' equation with an explicit finite elements method. Soil hydraulic conductivity and water diffusivity are calculated from the measured soil water retention curves of the soil layers using hydraulic functions (Mualem, 1976, van Genuchten *et al.*, 1992).

Only photosynthesis and stomatal conductance are directly dependent on CO_2 concentration. All other CO_2 responses of the crop follow from their functional dependence on these processes in the model. This is a simplification, since some variables such as the leaf area per unit leaf mass or the pattern for the distribution of assimilates to the different organs might change under elevated CO_2. Further experiments are necessary to clarify such questions and allow them to be quantified in models.

The main influence of soil water limitation on the productivity of the crop and the interaction of water limitation with the atmospheric CO_2 concentration is mediated by the canopy assimilation rate in the model. The model part for the integrated calculation of canopy assimilation rate and energy fluxes is therefore described in more detail than the other processes, for which we refer to the literature.

Energy fluxes, stomatal conductance and net assimilation rate
A 'big leaf' model (Shuttleworth, 1991) is used to calculate canopy temperature (T_c), water and energy fluxes between the canopy and the atmosphere. The assumption is made that the whole canopy is exposed to the same microclimate. Therefore, calculated CO_2 concentration, air temperature and water vapor pressure are taken as being constant throughout the canopy (Eqns A1–A8; all cited equations are given in the Appendix 1). The stability correction of the aerodynamic resistance is calculated according to Choudhury *et al.* (1986) for stable conditions and Mahrt & Ek (1984) for unstable conditions (Eqns A9–A11). Atmospheric emissivity (ε_a) which is necessary to calculate the long-wave radiation balance of the crop was determined according to Idso & Jackson (1969).

The light intensity profile is assumed to be the main cause of vertical variations of the assimilation rate and stomatal conductance inside the canopy (Raupach & Finnigan, 1988). In contrast to the calculation of the water and energy fluxes, leaf net assimilation rate and stomatal conductance are calculated for different layers inside the canopy contributing to the canopy net assimilation rate and canopy conductance (Eqns A12–A13). The thickness of the canopy layers is less than or equal to half a leaf layer to achieve sufficient accuracy in simulating canopy transpiration (Stockle, 1991). The model of Farquhar & von Caemmerer (1982) is used to calculate the assimilation rates for the sunlit and shaded leaf fractions of each layer as a function of the incoming photosynthetically active radiation, the CO_2 concentration in the chloroplasts (c_c) and canopy temperature (T_c) (Eqns A14–A22). Activation energies to describe the temperature response of the kinetic constants of Rubisco are taken from Long (1991). The values of the Michaelis–Menten constants for O_2 and CO_2 at reference temperature were obtained from data of von Caemmerer *et al.* (1994), who consider an internal leaf resistance (Eqn A20). This was necessary since the assimilation rates were determined by means of the CO_2 concentration in the chloroplasts (c_c). The temperature dependence of the potential rate of electron transport (J_{max}) is calculated according to Farquhar *et al.* (1980) (Eqn A21). Temporal changes of the parameters of the photosynthesis model, which are not caused by temperature, are described by changes in the leaf nitrogen content (Eqns A16, A19).

According to the approach of Goudriaan *et al.* (1985) and Jacobs *et al.* (1996) c_i is calculated from the ratio:

$$f = (c_i - \Gamma)/(c_s - \Gamma)$$

(c_s, the CO_2 concentration on the leaf surface; and Γ, CO_2 compensation point.) This approach accounts for the effects of cuticular conductance, day respiration, CO_2 concentration and the vapor pressure deficit of the air on the ratio of c_i to c_s (Eqns A25–A29).

Unlimited water supply

A coupled equation system containing the canopy energy balance equation (Eqn A29), the biochemical equations for determining the assimilation rates in each layer, the equations for calculating the various CO_2 concentrations, the micrometeorological variables inside the canopy and canopy conductance is solved for every simulation time step under the assumption of unlimited soil water supply. The energy balance equation of the canopy is an ordinary differential equation of the canopy temperature (T_c) and is solved by means of the Newton–Raphson iteration (Eqn A30). This procedure delivers the potential canopy transpiration rate (E_p).

Limited water supply

The sum of the uptake capacity of the roots of different soil layers determines the possible canopy transpiration rate (E_c). The uptake capacity is calculated by an empirical function depending on the root biomass, the activity of the roots and the soil water content (Groot, 1987, cp. paragraph 2.1.2). If E_c is lower than the potential transpiration rate (E_p) the energy balance equation is solved to calculate canopy temperature (T_c) energy fluxes and atmospheric state variables inside the canopy for the lower transpiration rate. Canopy conductance ($g_{s,c}$) is then determined from Eqn A1. The CO_2-concentration (c_c) with which the calculated canopy assimilation rate ($A_{n,c}$) provides the canopy conductance ($g_{s,c}$) is determined by means of the Newton–Raphson iteration using Eq A31 and Eq. A32, which is obtained by combining Eqn A13, A22 and A24. The iteration stops if the change in c_c is smaller than $0.1\ \mu mol\ mol^{-1}$. If the uptake capacity is very low, transpiration rate is determined by the canopy cuticular conductance. This procedure describes 'nonstomatal' effects on photosynthesis by the reduction of c_i due to soil water limitation.

Figure 1 gives a schematic overview of the description of drought in the model and its interaction with elevated CO_2 via the mechanisms listed in the 'Introduction'.

Effect of water limitation on growth processes The canopy temperature of wheat plants was shown to increase by up to 4K under soil water limitation (Seligman *et al.*, 1983), which has an effect on phenology, maintenance respiration and indirectly on growth via the temperature response of photosynthesis. The higher calculated canopy temperature is therefore used in the model DEMETER to describe the acceleration of the phenological development of the crop under soil water limitation.
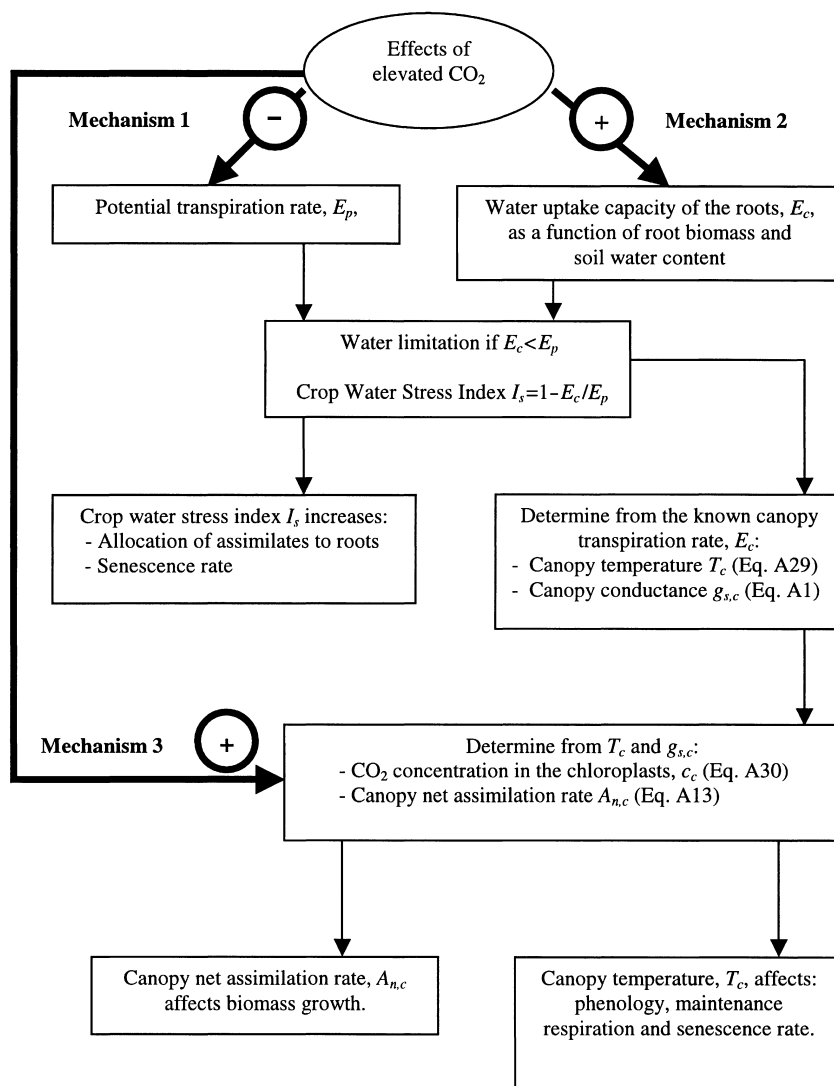
Fig. 1 Sequence of responses in the wheat model DEMETER initiated by soil water limitation and the interaction with elevated atmospheric CO_2 concentrations (mechanisms 1–3). Soil water limitation occurs in the model when the water uptake capacity of the roots (E_c) falls below the potential transpiration rate (E_p).

The water uptake capacity of the roots in the different soil layers is modelled according to Groot (1987) as an empirical function of the root biomass and the relative soil water content (W_r), which is given by $(W_c − W_p)/(W_f − W_p)$ with W_c, W_f and W_p being soil water content, field capacity and wilting point of the different soil layers, respectively. The uptake capacity is reduced with decreasing soil water contents beneath a threshold value of $W_r = 0.5$ as a stepwise linear function.

The crop water stress index (I_s) is used to describe the effect of drought on senescence rate and root growth. It is effective only if it reaches a threshold value of 0.6, which is usually accomplished after a longer period of water limitation. This expresses the fact that short-term drought only affects stomatal conductance, photosynthesis and phenology directly and stops when the soil is sufficiently refilled with water. Drought can double the senescence rate.

In the case of soil water limitation the allocation pattern of assimilates is changed in favour of the root biomass. After distributing the standard amount of assimilates to the roots, the remainder is multiplied by I_s and this amount of assimilates is available for root growth.

Grain yield is influenced by soil water limitation in the model through the shortening of the grain filling period and the reduction of the carbohydrate flow.

Simulation experiment The model DEMETER was applied from 12 January to 15 May 1993 and from 4 January to 15 May 1994. Simulations were made for CO_2 mole fractions of 360 µmol mol^{-1} (ambient) and 550 µmol mol^{-1} (FACE) for both growing seasons.

The measured hourly air temperature, humidity and wind velocity at 2 m reference height, solar radiation, precipitation, as well as fertilizer and irrigation treatments were used as input data for the model. Site-specific data for the physical characteristics of the soil (saturated hydraulic conductivity, wilting point, field capacity, albedo, particle density, heat

Parameter	Symbol	Value	Units
Emissivity of the leaves	ε_c	0.96	(–)
Emissivity of the soil	ε_s	0.96	(–)
Soil reflectance of near infra-red radiation	α_{nir}	$2\alpha_{par}$	(–)
Leaf scattering coefficients for visible and near infra-red radiation	σ_{par}	0.8	(–)
	σ_{nir}	0.2	(–)
Maximum crop height	h_{max}	1.0	m

Table 1 Parameter values used in the model for the simulations if not stated in Appendix 2 'Definition of symbols'. A spherical leaf angle distribution is assumed. Soil reflectance for the visible part of the incoming solar radiation, α_{par}, depends on the soil water content of the first soil layer according to Dickinson *et al.* (1986)

capacity of the soil) were taken from Kimball *et al.* (1993). The RETC code of van Genuchten *et al.* (1992) was applied to fit the soil water retention curve through the data points. The applied drip irrigation was modelled by means of a water source at a soil depth of 0.2 m, which could be enriched with fertilizer. All state variables and rates were calculated for every hour for the entire growing season.

As observed in the FACE-experiments the phenological development of the plants grown under elevated CO_2 was accelerated significantly by the effect of the blowers (Pinter *et al.*, 2000). This phenomenon is difficult to model and therefore measurements of the phenological stages of the crop according to Zadoks (Zadoks *et al.*, 1974) were used as input data in the simulations.

Results of Garcia *et al.* (1998) revealed that the stomata of this particular wheat variety do not respond to the specific humidity deficit at the leaf surface. A direct response of the stomata to the specific humidity deficit at the leaf surface was therefore not considered in the model.

In the simulations, model parameters for spring wheat available in the scientific literature were used (cp. paragraph 2.2). An exception had to be made for the ratio of leaf mass per unit leaf area, which is the basis for the calculation of the leaf area index and a key parameter in crop growth models. A typical value for this ratio for spring wheat is 0.05 kg m^{-2} (Penning de Vries *et al.*, 1989). This value differs considerably from the measurements at the beginning of the season during the FACE-wheat experiments (0.03 kg m^{-2} for 1993 and 0.06 kg m^{-2} for 1994, respectively). Different values for leaf mass per unit leaf area had to be used in the model simulations for the two seasons (0.04 kg m^{-2} for the year 1993 and 0.05 kg m^{-2} for the year 1994). Table 1 contains parameter values used in the model for the simulations other than specified in Appendix 2.

Results and Discussion

Biomass and yield

The seasonal courses of the simulated and measured *green biomass* (sum of leaf and stem mass and mass of the nongrain portion of ear) and the standard deviations for the four treatments (FACE wet, ambient wet, FACE dry, ambient dry) of the 1993 and 1994 FACE runs are shown in Figs 2 and 3. The

model overestimated the productivity of the crop significantly in March 1993 and 1994 for all treatments as well as in April 1994 for the two FACE treatments. It is interesting to mention that the simulations reflect well the behaviour of the replicate with the highest measured values of green biomass. Plants in this replicate might have experienced the closest to ideal growth conditions, which are assumed in the model. Tubiello *et al.* (1999) and Grant *et al.* (1999) also reported an overestimation of the simulated biomass for the same treatments.

The differences between the measured and the simulated values might be caused further by deviations in the allocation pattern for assimilates, which was obtained from the literature for spring wheat in general and not adapted for the particular variety. The simulated green biomass is also sensitive to the parameterization and scaling methods of the model for the integrated calculation of canopy assimilation rate, stomatal conductance and energy fluxes, which is discussed in paragraph 3.2. The soil characteristics used in the model might be inaccurate due to inhomogeneities of the soil at the experimental site. This can cause differences in the simulated amount of the water available for the plants. Furthermore, a water-saturated soil was assumed at the beginning of the simulations for both years, which might overestimate the soil water content in the model for the 1994 season. The crop received a high amount of irrigation water prior to emergence in 1993 (371 mm), but only about 40 mm in 1994.

To illustrate the CO_2 effect on the green biomass, the percent change of the measured and simulated values due to elevated atmospheric CO_2 for the wet and the dry treatments of the two years are given in Fig. 4. Drought was detected after the beginning of March in 1993 and after the end of February in 1994 in the model. Late in the season, the blower effect (Pinter *et al.*, 2000) led to differences in biomass due to the acceleration of the senescence rate of the FACE treatments rather than elevated CO_2. This explains the decline in the CO_2 effect on green biomass in April of the two growing seasons. After the onset of drought, the simulations show a consistently higher CO_2 effect on the green biomass for the dry treatments of about 8% in 1993 and 15% in 1994 (Fig. 4a,b). The picture is less clear for the experimental data, but a higher CO_2 effect on the green biomass under water limitation was detected for most of the data points of the two growing seasons. Between the first occurrence of water limitation and the end of April, the CO_2 effect on the green
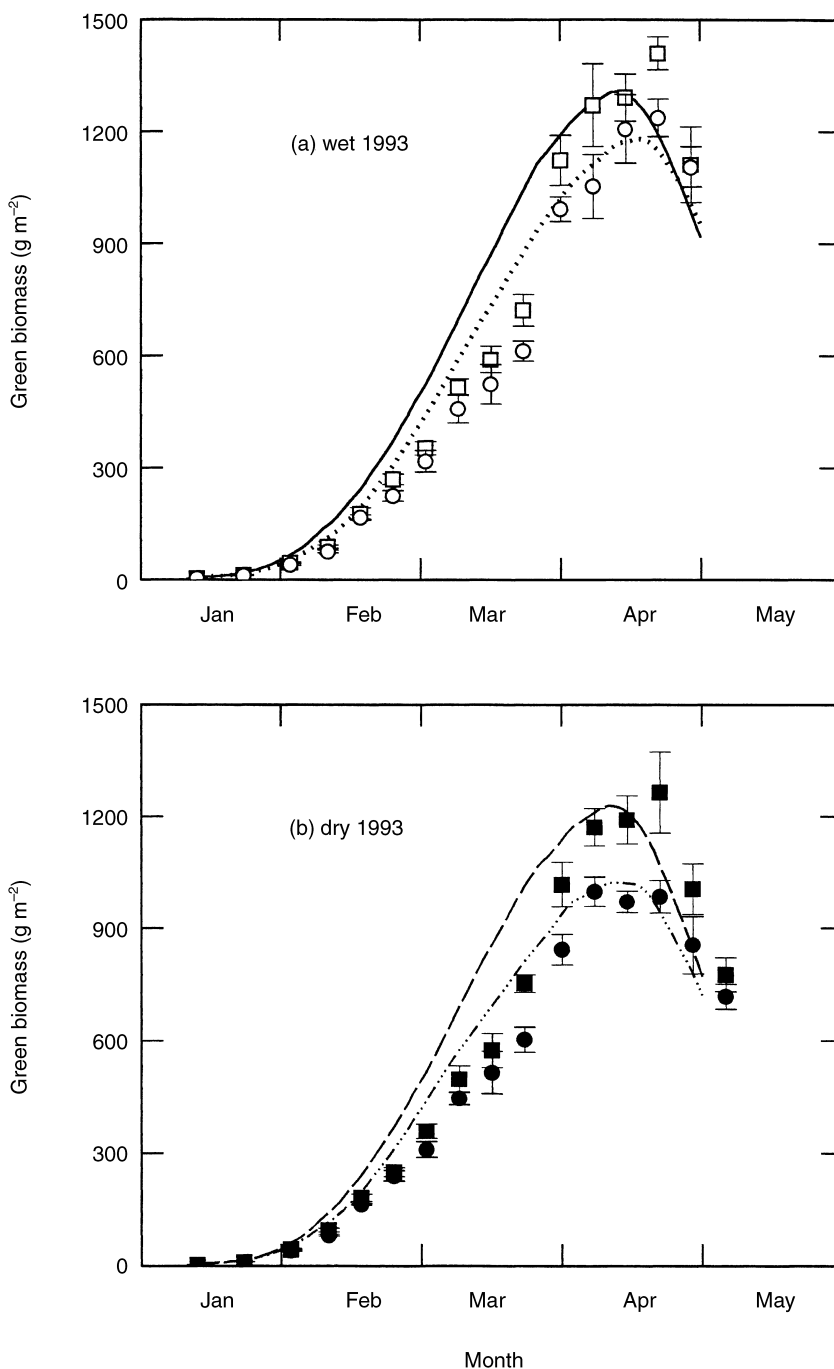
Fig. 2 Simulated and measured green biomass (sum of leaf and stem mass and mass of the nongrain portion of the ear) for the 1993 growing season for spring wheat grown under: (a) Well watered conditions and a CO_2 mole fraction of 550 µmol mol^{-1} (open squares, measured; solid line, simulated) and well watered conditions and ambient CO_2 (open circles, measured; dotted line, simulated); (b) Soil water limitation and a CO_2 mole fraction of 550 µmol mol^{-1} (closed squares, measured; dashed line, simulated) and soil water limitation and ambient CO_2 (closed circles, measured; dashed and dotted line, simulated).

biomass for the dry treatments was on average 6% higher than the wet treatments in 1993 and 13% higher in 1994.

At the end of the grain filling period the *grain biomass* for the 1993 growing season was measured to be 0.92 ± 0.04 kg m^{-2}, 0.83 ± 0.04 kg m^{-2}, 0.90 ± 0.06 kg m^{-2} and 0.67 ± 0.08 kg m^{-2} for the FACE wet, ambient wet, FACE dry and ambient dry treatments. The simulated values for the same treatments were 0.95 kg m^{-2}, 0.85 kg m^{-2}, 0.90 kg m^{-2} and 0.72 kg m^{-2}, which is in good agreement with the measurements. This translates to a CO_2 effect of 12 and 15% for the measurements and the

simulations, respectively, under unlimited water supply and the higher values of 25 and 34% under water limitation. The measured and simulated values for the different treatments of the 1994 growing season were 0.86 ± 0.02 kg m^{-2}, 0.76 ± 0.07 kg m^{-2}, 0.74 ± 0.08 kg m^{-2}, 0.62 ± 0.03 kg m^{-2}, and 0.97 kg m^{-2}, 0.87 kg m^{-2}, 0.82 kg m^{-2} and 0.61 kg m^{-2}. The CO_2 effect was measured and simulated to be 10 and 12% for the wet, and 20 and 34% for dry treatments. The CO_2 effect on grain mass is clearly higher under water limitation for both the measured and the simulated results.
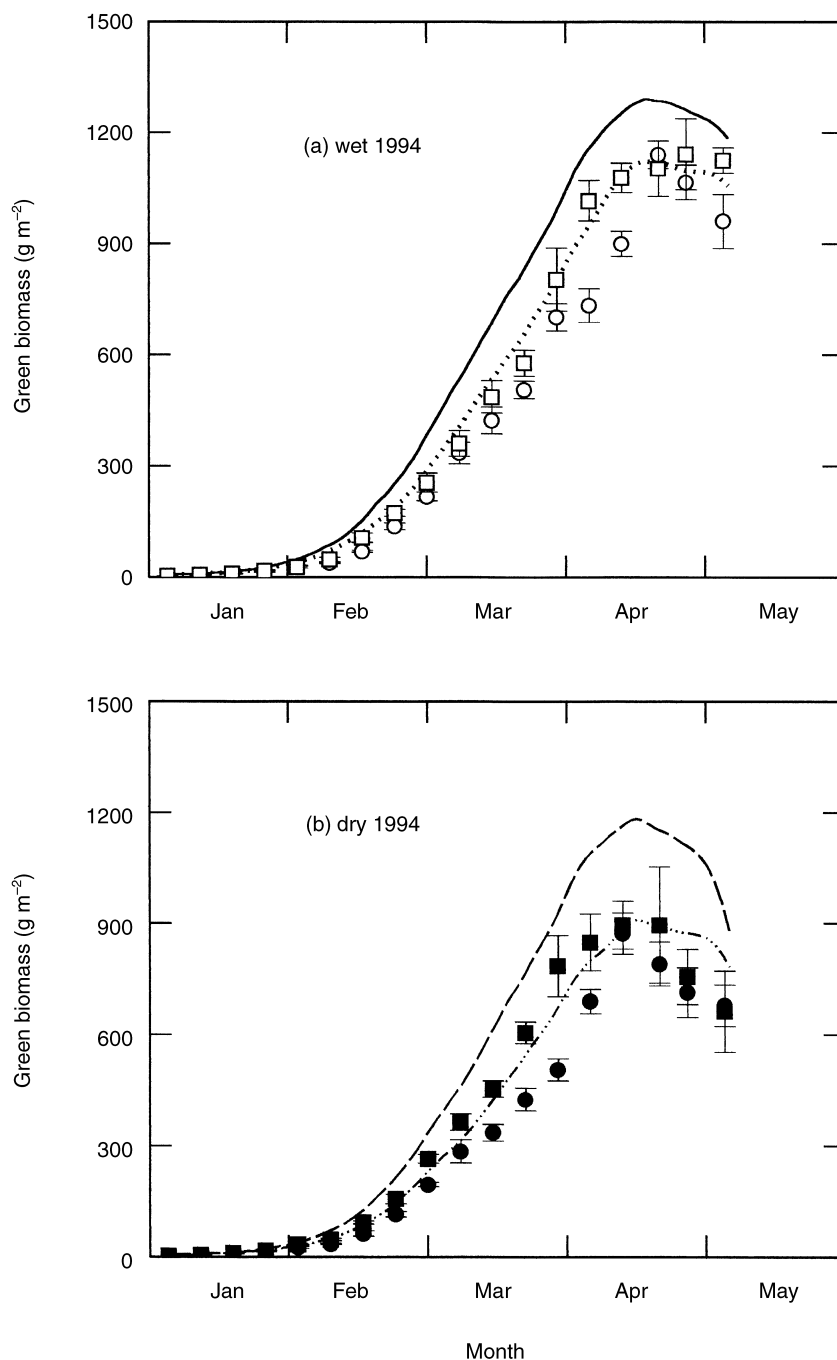
Fig. 3 Simulated and measured green biomass (sum of leaf and stem mass and mass of the nongrain portion of the ear) for the 1994 growing season for spring wheat grown under: (a) Well watered conditions and a CO_2 mole fraction of 550 µmol mol^{-1} (open squares, measured; solid line, simulated) and well watered conditions and ambient CO_2 (open circles, measured; dotted line, simulated); (b) Soil water limitation and a atmospheric CO_2 mole fraction of 550 µmol mol^{-1} (closed squares, measured; dashed line, simulated) and soil water limitation and ambient CO_2 (closed circles, measured; dashed and dotted line, simulated).

Canopy transpiration and energy fluxes It was shown in a previous paper (Grossman-Clarke *et al.*, 1999) that the simulated cumulative sum of canopy transpiration (E_c) and soil evaporation (E_s) for the wet treatments in 1993 was reduced by *c.* 5% under elevated CO_2. This was in close accordance with the measured value of 8%, which was obtained from the soil water balance method (Hunsaker *et al.*, 1996). A similar result was found for the wet treatments of the 1994 growing season (Fig. 5), where the simulated cumulative sum of E_c and E_s was reduced by *c.* 4% due to elevated CO_2. This corresponds

closely with the measured value of 3.3%. The measurements of E_c and E_s for each treatment are averages of the four replicates with standard deviations of 30–50 mm at the end of the growing season. The simulation results were in agreement with the measurements for the whole growing season, which can be explained by the fact that the simulation results for the wet treatments after canopy closure (occurring relatively early in the season) are almost independent from deviations between the measured and simulated LAI and also from the simulated root biomass.
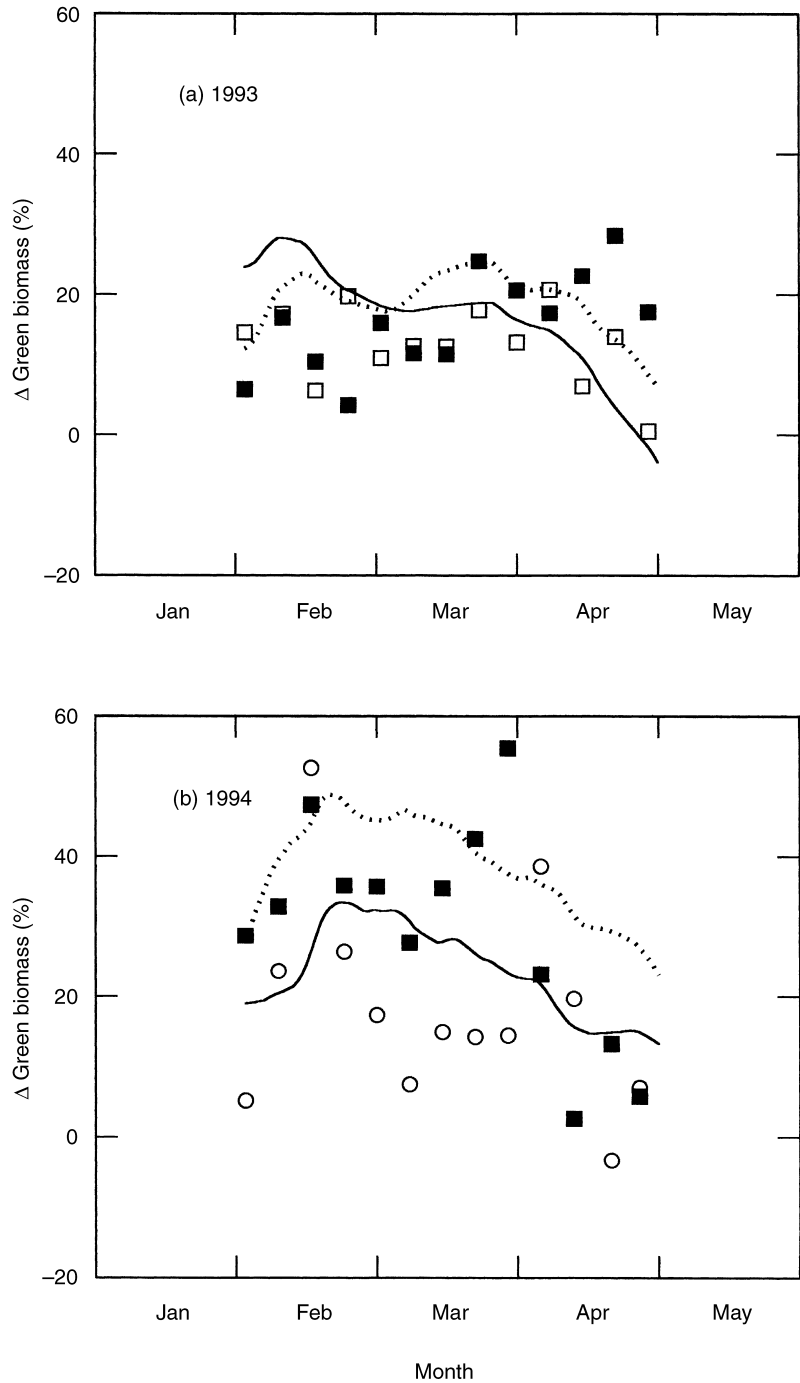
Fig. 4 Simulated and measured relative CO_2 effect on the green biomass in percent (sum of leaf and stem mass and mass of the nongrain portion of the ear) for: (a) Wet treatments (open squares, measured; solid line, simulated) and dry treatments (closed squares, measured; dotted line, simulated) of the 1993 growing season; (b) Wet treatments (open squares, measured; solid line, simulated) and dry treatments (closed squares, measured; dotted line, simulated) of the 1994 growing season.

Canopy transpiration was obtained from the hourly solution of the canopy energy balance equation in the model. The differences between measured and simulated hourly latent and sensible heat fluxes (λE and H), net radiation (R_n) and canopy temperature (T_c) vs. the measured values are presented for 9 d in 1993 and 4 d in 1994 for the ambient and FACE wet treatments in Figs 6 and 7, respectively. All simulated fluxes are the sum of soil and canopy fluxes. Net radiation is assumed to be positive if directed towards the canopy, whereas turbulent heat fluxes are positive in the model if directed away from the canopy. The measured data points are averages of the data obtained from the four replicates with standard deviations less than 40 W m^{-2}. The small fetch length for the measurements introduced an additional uncertainty of ± 50 W m^{-2} in the measured values for the turbulent heat fluxes (Kimball *et al.*, 1999).

The average correlation coefficient (r^2) between measured and simulated ambient and FACE values, as determined from
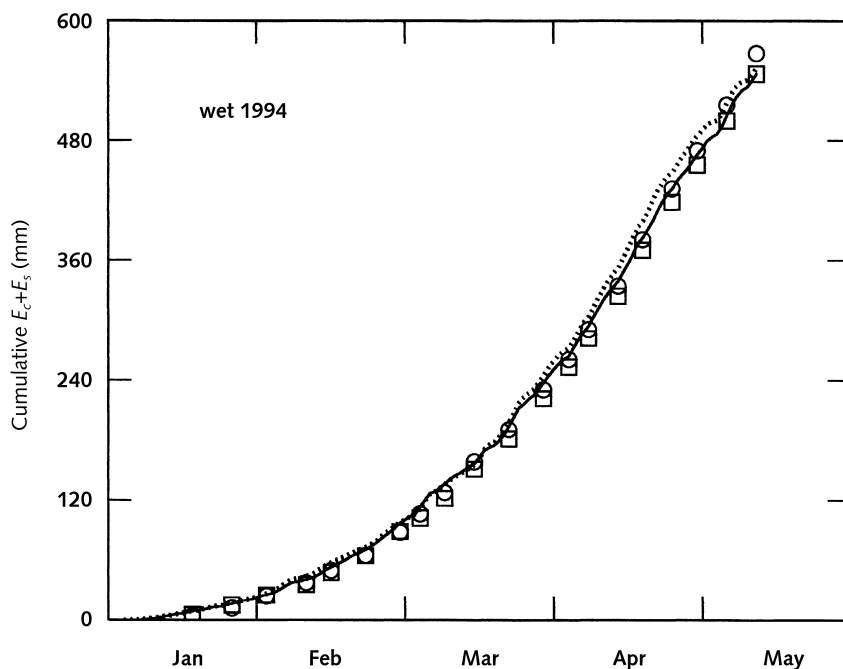
Fig. 5 Cumulative sum of canopy transpiration (E_c) and soil evaporation (E_s) of a wheat crop grown under unlimited water supply and ambient CO_2 (open circles, measured; dotted line, simulated) and an atmospheric CO_2 concentration of 550 µmol mol⁻¹ (open squares, measured; solid line, simulated) for the 1994 growing season.

the linear regression analysis is 0.99, 0.97, 0.78 and 0.98 for R_n, λE, H and T_c, respectively, which illustrates the quality of the simulations for the cumulative sum of E_c and E_s for the wet plots. Deviations between measurements and numerical results can arise from the model approaches used and their parameterization. The simulated net radiation balance (R_n) is significantly influenced by the approach used for determining the atmospheric emissivity (ε_a). A systematic underestimation of the incoming long-wave radiation from the sky explains the large deviations between measured and simulated temperatures during cold nights (Figs 6d and 7d).

The simulations show relatively high deviations from the measurements for the sensible heat fluxes (H), which is typical (Leuning *et al.*, 1998) since H is determined from the difference in air and canopy temperature (T_c) in the model (Figs 6b and 7b). Small changes in T_c can therefore lead to relatively high errors in the simulated sensible heat fluxes.

Strong deviations (> 100 W m⁻²) between the simulated and measured H and λE occurred on 2 days of the 1994 growing season, which were characterized by a high incoming solar radiation but relatively low latent heat fluxes. This indicates water limitation for the crop, which was not detected by the model and resulted in an overestimation of λE and an underestimation of H. In late afternoons, the aerodynamic resistance (r_a) was occasionally underestimated by the model leading to an overestimation of the turbulent heat fluxes.

Most of the simulated data for λE differ < 100 W m⁻² from the measurements. The simulated latent heat fluxes are sensitive to the simulated canopy assimilation rate ($A_{n,c}$).

The maximum carboxylation capacity (V_{cmax}) is obtained from a typical value for the proportion of the leaf nitrogen

content in the rubisco protein (f_{rub}) (Eq. A16), which is, according to Evans (1989), about 0.23 for wheat leaves. Seasonal changes of the leaf nitrogen content were included in the simulations (van Keulen & Seligman, 1987), but the assumption of an unchanged value of f_{rub} for the whole growing season might be inaccurate and can lead to errors in the simulated canopy assimilation rate. Osborne *et al.* (1998) showed for this particular wheat crop that f_{rub} was reduced with increasing depth in the canopy, whereas the proportion of the leaf nitrogen in the light-harvesting-complex (LHC) protein increased under elevated CO_2. This acclimation of the photosynthetic apparatus led to a vertically unchanged value for the potential rate of electron transport (J_{max}). Such detailed information is usually not available from standard measurements and not considered in models, since causality is not known. The simulation results for λE are influenced further by the approach for the calculation of the electron transport rate. In DEMETER the equations of Farquhar & Wong (1984) are used.

The method of scaling leaf stomatal conductance and assimilation rate to plant and canopy levels can be important for the quality of the simulations. In our model the nonlinear dependence of assimilation rate on the absorbed radiation is accounted for by calculating leaf assimilation rate for shaded and sunlit leaves in separate canopy layers. On the other hand, assimilation rate is also nonlinearly related to leaf temperature and internal CO_2 concentration (c_i). We used only one value for c_i and T_c for all leaves in the canopy, which might have introduced inaccuracy in the simulated values of $A_{n,c}$ and $g_{s,c}$

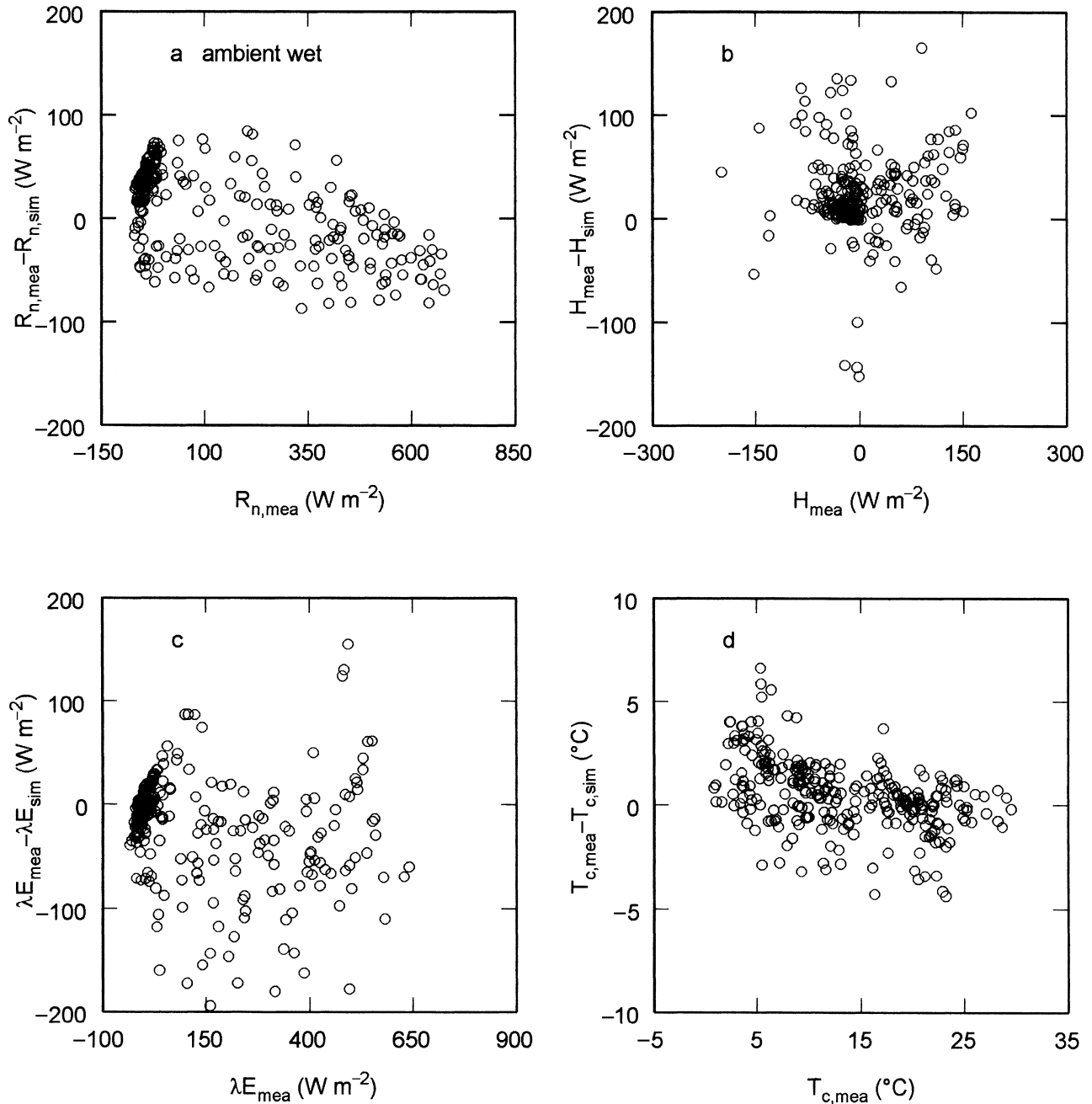Introducing more detail into the model equations would significantly increase the computation time. The accuracy of

Fig. 6 Residual (measured minus simulated) values of hourly net radiation (R_n) sensible heat flux (H) latent heat flux (λE) and canopy temperature (T_c) vs. measured values for the ambient wet treatments for 9 d and 4 d of the growing seasons 1993 and 1994, respectively.

this part of the wheat growth model must be balanced with possible inaccuracies of other approaches. Our approach can be justified somewhat by the results of Baldocchi (1993) who, by comparing simulation results from a detailed Lagrangian random-walk model with a model that assumes a constant CO_2 profile within the canopy, showed that 'scaling of CO_2 uptake by an aerodynamically smooth crop with a high photosynthetic capacity requires an accurate radiative transfer model to calculate the electron transport-limited rate of

photosynthesis for the shaded leaves and an accurate model of turbulent transfer to calculate the RuBP-saturated carboxylation rate well for the sunlit leaves'. 'Big-leaf' models with various levels of detail were shown to work sufficiently well (Amthor *et al.*, 1994; de Pury & Farquhar, 1997; Wang & Leuning, 1998; Grant *et al.*, 1999).

Deviations between measurements and simulations might further be caused by simplifications in the model DEME-TER, which exclude the observed delay of hours in the
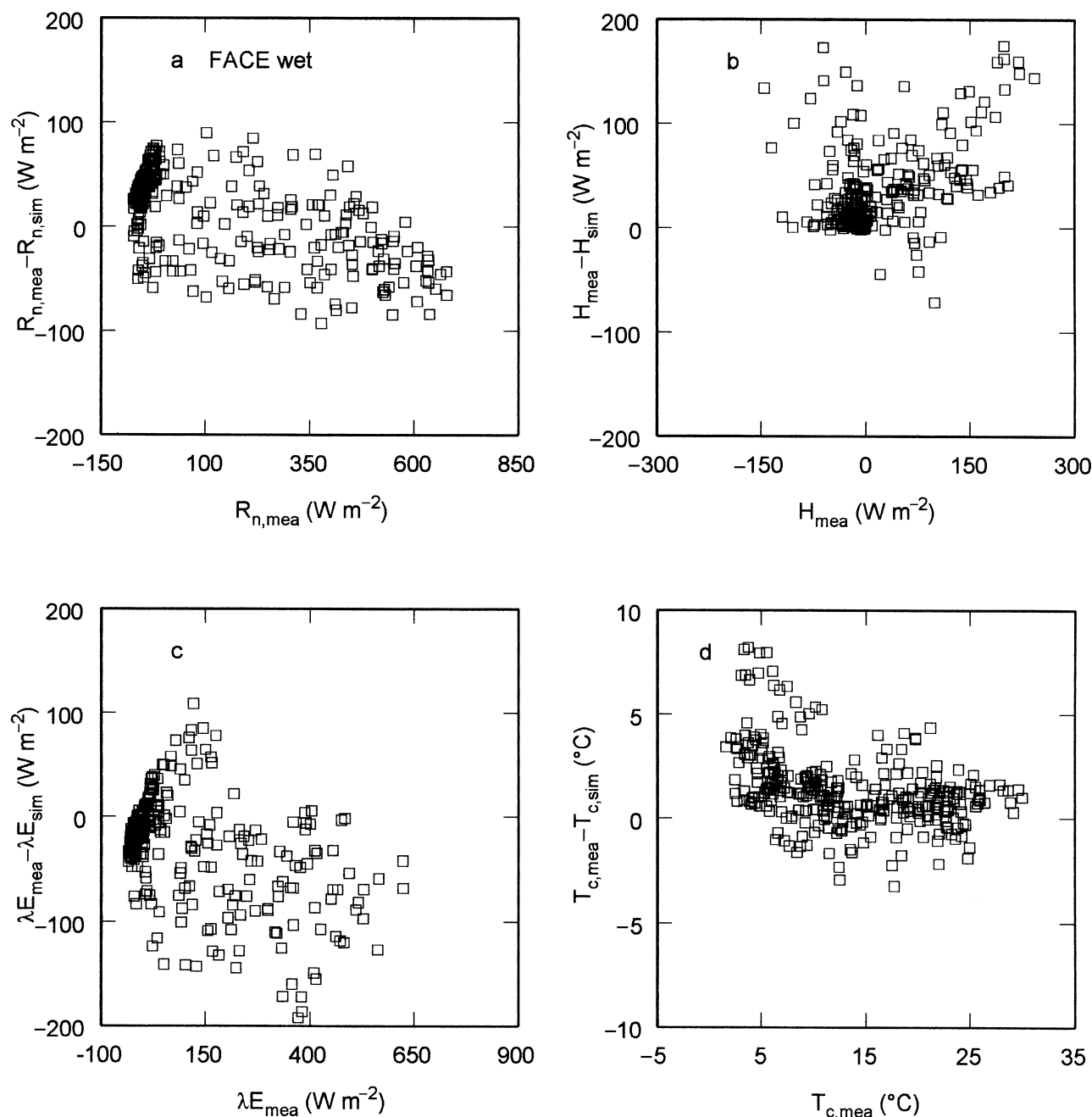
Fig. 7 Residual (measured minus simulated) values of hourly net radiation (R_n) sensible heat flux (H) latent heat flux (λE) and canopy temperature (T_c) vs. measured values for the FACE wet treatments for 9 d and 4 d of the growing seasons 1993 and 1994, respectively.

opening of the stomata after rewatering, despite a normalized turgor potential (Raschke, 1987) or the condition of an extremely dry soil (the assumption of water-saturated air inside the leaves is not fulfilled). Also not considered in the model are 'nonstomatal' effects of water limitation on assimilation rate, which might decrease the maximum value of g_s irreversibly by reducing photosynthetic capacity after severe water stress (Raschke, 1987; Tenhunen *et al.*, 1987; Cornic, 1994).

The energy fluxes of the dry treatments were not measured

since the fetch length of the plots was too small. However, the cumulative sum of canopy transpiration and soil evaporation was determined. The agreement between the measurements and the simulations is not quite as good as for the wet treatments (Fig. 8a,b), since deviations between the measured and simulated green biomass and root biomass can affect the results significantly. Differences in the cumulative sum of E_c and E_s due to elevated CO_2 were not simulated for the dry treatments of the 1993 growing season, but the measurements
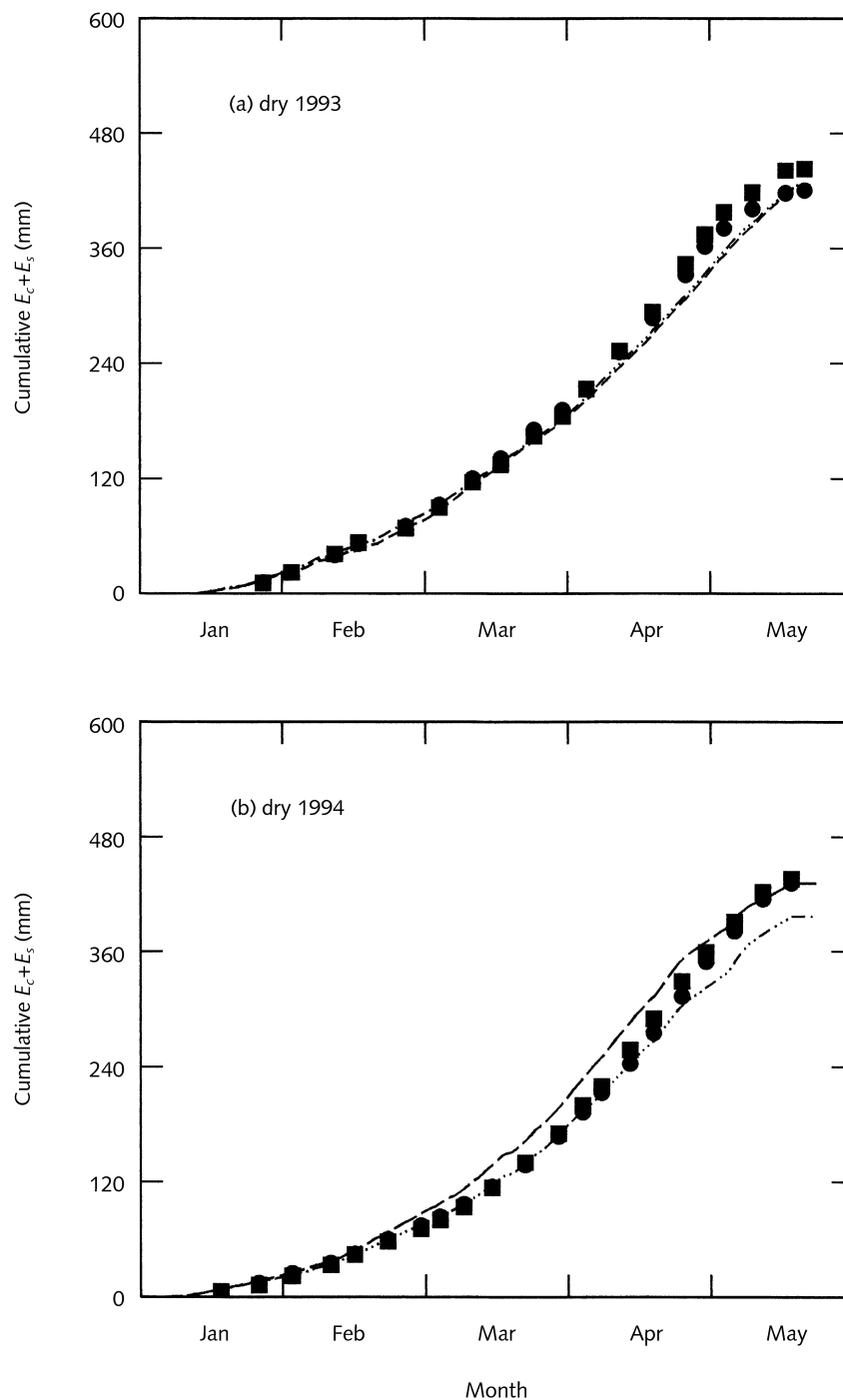
Fig. 8 Cumulative sum of canopy transpiration (E_c) and soil evaporation (E_s) of spring wheat, grown under limited water supply for: (a) Ambient atmospheric CO_2 (closed circles, measured; dashed and dotted line, simulated) and a CO_2 mole fraction of 550 μmol mol^{-1} (closed squares, measured; dashed line, simulated) for the 1993 growing season; (b) Ambient atmospheric CO_2 (closed circles, measured; dashed and dotted line, simulated) and a CO_2 mole fraction of 550 μmol mol^{-1} (closed squares, measured; dashed line, simulated) for the 1994 growing season.

show a 4% higher cumulative sum of canopy transpiration and soil evaporation for the FACE dry treatment at the end of the growing season. The cumulative sum of E_c and E_s was overestimated for the FACE dry treatment in 1994 leading to a 4% increase due to elevated CO_2. No significant differences were detected during the measurements for the same treatments.

The results show only slight CO_2-induced differences in the seasonal sum of canopy transpiration and soil evaporation,

which depend on the additional biomass growth. A weak but consistent tendency toward reduced water use under elevated CO_2 was measured and simulated for potential growth conditions, despite the CO_2-induced biomass increase. The biomass increase was greater when soil water was limiting so that water use under elevated CO_2 was unchanged or higher. An exact prediction of the differences in water use seems to be difficult because of the inaccuracies in the biomass predictions.

Interactions of elevated atmospheric CO$_2$ and water limitation
The simulated CO$_2$ effect on canopy assimilation rate and stomatal conductance for the different CO$_2$ and irrigation treatments was determined at 12 : 00 noon on selected days of the two growing seasons, which were characterized by a relatively high water stress index (I_s). The influence of a particular cause for the higher CO$_2$ effect under water limitation was investigated by eliminating the influence of the other causes and analysing to what degree this changed the simulation results.

Potential transpiration On a canopy level the potential transpiration rate (E_p) might be lower under elevated CO$_2$ if the increase in biomass due to elevated CO$_2$ does not compensate for the decrease in transpiration rate per unit leaf area due to CO$_2$-induced stomatal closure. The simulated potential transpiration was smaller for all FACE treatments compared with the corresponding ambient treatments of the two growing seasons despite the aboveground biomass increase.

Therefore the crop water stress index (I_s) acting on root biomass and senescence rate was lower for the FACE dry than for the ambient dry treatments. To investigate the influence of a higher I_s under ambient dry conditions on the results, I_s was assumed to be zero in the simulations. This assumption led to an even higher CO$_2$ effect on $A_{n,c}$ under water limitation since the ambient dry treatment did not obtain the additional assimilates for root growth in proportion to the higher I_s.

According to the model, the ability of the crop to fulfil E_p and therefore maintain an unstressed situation lasted longer in the FACE treatments because of the longer period of unlimited water availability in the soil. Soil water limitation occurred 9 days later in the FACE dry than in the ambient dry treatment.

The simulated potential stomatal conductance and therefore assimilation rate could be fulfilled in the FACE dry treatments to a higher degree than in the ambient dry treatments. To investigate the amount of this influence on the overall simulated CO$_2$ effect under water limitation, $A_{n,c}$ and $g_{s,c}$ were first calculated with the ambient atmospheric CO$_2$ concentration. The CO$_2$ mole fraction was than set to 550 μmol mol^{-1} for 12 : 00 noon of the selected days. This excluded long-term differences in soil water content, root biomass and green biomass between FACE and ambient conditions and at the same time did not have a significant feedback on these variables. Differences in E_p were therefore only caused by the different CO$_2$ concentrations. The simulations showed that the lower value of E_p accounted for only 30–50% of the higher CO$_2$ response of the assimilation rate under soil water limitation during vegetative growth, when soil water contents were not very low and transpiration demands were not very high. The remaining 50–70% of the response must therefore be attributed to the higher root biomass of the FACE plants and the nonlinear functional dependence of the assimilation rate on c_i. After prolonged drought during reproductive growth the soil water contents were very low. At that time the lower E_p

accounted for up to 70% of the higher CO$_2$ effect under soil water limitation. In the model this was due to the fact that the uptake capacity of the roots strongly decreases at low soil water contents despite the CO$_2$ induced increase in root biomass. Also at higher transpiration demands later in the season the reduction of E_p due to elevated CO$_2$ was more pronounced.

Nonlinearity of the A_n-C_i cursive The advantage of a lower potential transpiration rate and higher water availability under elevated CO$_2$ compared with ambient conditions was strengthened significantly by the nonlinear functional dependence of the net assimilation rate on the leaf internal CO$_2$ concentration in the model. Assimilation rate levels off with increasing CO$_2$ concentrations (second derivative of Eqn A14 in terms of c_c is negative, c_c can be replaced in this example by c_i). That means that the same relative reduction of the canopy conductance or leaf internal CO$_2$ concentration due to drought leads to a higher reduction of the assimilation rate under ambient than under FACE conditions. For example, a 78% reduction of the canopy conductance due to drought, as experienced by the ambient plants at 12 noon of 11 April 1993, led to a 47% reduction of the assimilation rate of the ambient treatment, but only to a 42% reduction of the assimilation rate of the FACE plants in the model. Assuming the change in assimilation rate of 42% for the ambient plants reduced the higher CO$_2$ effect under water limitation by 30%. The range of the contribution of the nonlinear functional dependence of A_n on c_i in the model to the higher CO$_2$ effect under soil water limitation was 20–30% and increased with a higher crop water stress index.

Root biomass The higher root biomass caused by elevated CO$_2$ led to a higher water uptake capacity in the model for the FACE treatments, which was more significant during vegetative growth, when soil water contents were still not very low. At that time the higher root biomass of the FACE plants accounted for up to 50% of the higher CO$_2$ response of the assimilation rate under soil water limitation.

In Table 2 the measured (taken from Wechsung *et al.*, 1999; Table 1) and simulated values of the root biomass for a soil depth of 0–1 m for 5 dates for the wet treatments of the 1993 growing season are shown. Only two data points were available from the measurements for the dry treatments. The measured data are averages obtained from 'in row' and 'inter row' sample positions. The measured CO$_2$ effect on root biomass was higher during vegetative than during reproductive growth for the wet treatments. At anthesis the measured and simulated CO$_2$ effect was more pronounced for the dry treatments. This was due to the stronger reduction of assimilation rate due to water limitation of the ambient dry than of the FACE dry treatments and therefore the reduced supply of assimilates to the roots for the ambient dry treatment. The model overestimated the root biomass for all treatments and underestimated the CO$_2$ effect for most of the data points.

Table 2 Measured (taken from Wechsung *et al.*, 1999, Table 1) and simulated values of root biomass (g m^{-2}) for the 1993 growing season. Measured data for 5 dates (16, 36, 63, 92, 113) are available for the ambient and FACE wet treatments, but only for 2 dates for the dry treatments. The measured data are averages obtained from 'in row' and 'inter row' sampling positions. The measured data are underlined

Treatment	Three leaf stage (16)	Tillering (36)	Stem elongation (63)	Anthesis (92)	Dough development (113)
Ambient wet	3.6/14.0	15.7/32.9	56.2/91.1	85.3/101.1	67.0/93.0
FACE wet	5.0/14.0	20.8/37.0	73.2/99.8	85.7/105.1	84.7/96.5
Ambient dry	–/13.9	–/33.3	–/93.1	78.9/119.8	80.7/111.4
FACE dry	–/14.0	–/35.9	–/101.7	89.8/127.7	99.1/121.3
CO_2 effect (%)	wet: 38/0	wet: 32/12	wet: 30/10	wet: 0/4	wet:.26/4
	dry: –/0	dry: –/8	dry: –/9	dry: 14/7	dry: 24/9

However, the advantage of a higher root biomass of the FACE plants was reduced after prolonged water stress, when soil water contents and consequently the water uptake capacity of the roots were very low. The uptake capacity of the roots is a nonlinear function of the soil water content in the model. Therefore, the same percent increase in root biomass due to elevated CO_2 increases the water uptake capacity to a greater extent if water availability is higher. The higher root biomass of the FACE plants accounted for less than 10% of the higher CO_2 response of the assimilation rate under soil water limitation during reproductive growth.

Conclusions

The model DEMETER was able to describe the qualitative as well as the quantitative behaviour of a spring wheat crop under soil water limitation in comparison with an unlimited water supply for ambient vs a CO_2 mole fraction of 550 μmol mol^{-1}. This makes it possible to use the model with higher confidence for predictions about the future behaviour of spring wheat crops.

The model offered the opportunity to investigate the quantitative contributions of different mechanisms leading to a higher CO_2 effect on primary productivity and yield under soil water limitation in comparison with an unlimited water supply. The different mechanisms contributed with changing significance during the growing season of the crop. 30–50% of the higher CO_2 effect under water limitation during vegetative growth and up to 70% during reproductive growth, when soil water contents were very low and transpiration demands high, resulted from the lower potential transpiration rate of the FACE plants compared with that of the plants grown under ambient CO_2. The nonlinear dependence of net assimilation rate on leaf internal CO_2 concentration accounted for 20–30% of the difference throughout the season. The higher root biomass of the FACE treatments accounted for up to 50% of the difference in the CO_2 effect under water limitation compared to unlimited water supply during vegetative growth, but by less than 10% after prolonged drought, when water contents were very low, because of the reduced water uptake capacity of the roots.

The results of our study show that a well-tested simulation model can be a useful tool in understanding the complex interactions underlying observed ecosystem responses to drought. But there are limitations to the interpretation of the model results. Those limitations are based on the fact that models can reflect only potential behaviour, which is included in the equations and their parameterization. Frequently, facts known from experiments are omitted in models if they are considered insignificant for the model output, or not well enough understood to be described mathematically.

References

Allen LH, JrValle RR, Mishoe JW, Jones JW. 1994. Soybean leaf gas-exchange responses to carbon dioxide and water stress. *Journal of Agronomy* **86**: 625–636.

Amthor JS. 1999. Increasing atmospheric CO_2 concentration, water use, and water stress: scaling up from the plant to the landscape. In: Luo Y, Mooney HA, eds. *Carbon dioxide and environmental stress.* San Diego, CA, USA: Academic Press, 33–59.

Amthor JS, Goulden ML, Munger JW, Wofsy SC. 1994. Testing a mechanistic model of forest-canopy mass and energy exchange using eddy-correlation: carbon dioxide and ozone uptake by a mixed oak-maple stand. *Australian Journal of Plant Physiology* **21**: 623–651.

Asseng S. 1989. *Wurzelwachstumsmodell für Winterweizen.* Berlin, Germany: Humboldt-Universität zu Berlin, Fachbereich Pflanzenbau.

Baldocchi DD. 1993. Scaling water and carbon exchange from leaves to canopy: rules and tools. In: Ehleringer J, Field CB, eds. *Scaling physiological processes: leaf to globe.* London, UK: Academic Press, 77–114.

Choudhury BJ, Reginato RJ, Idso SB. 1986. An analysis of infrared temperature observations over wheat and calculation of latent heat flux. *Agricultural and Forest Meteorology* **37**: 75–88.

Clark H, Newton PCD, Barker DJ. 1999. Physiological and morphological responses to elevated CO_2 and soil moisture deficit of temperate pasture species growing in an established plant community. *Journal of Experimental Botany* **50**: 233–242.

Cornic G. 1994. Drought stress and high light effects on leaf photosynthesis. In: Baker NR, Bowyer JR, eds. *Photoinhibition of photosynthesis from molecular to the field.* Oxford, UK: Bios Scientific Publication, 297–313.

Cure JD, Acock B. 1986. Crop responses to carbon dioxide doubling: a literature survey. *Agricultural and Forest Meteorology* **38**: 127–145.

Daeter W, Hartung W. 1995. Stress-dependent redistribution of abscisic acid (ABA) in *Hordeum vulgare* L. leaves: the role of epidermal ABA metabolism, tonoplastic transport and the cuticle. *Plant, Cell & Environment* **18**: 1367–1376.

Daley PF, Raschke K, Ball JT, Berry JA. 1989. Topography of photosynthesis activity of leaves obtained from video images of chlorophyll fluorescence. *Plant Physiology* **90**: 1233–1238.

Davies WJ, Zhang J. 1991. Root signals and the regulation of growth development of plants in drying soil. *Annual Review of Plant Physiology and Molecular Biology* **42**: 55–76.

De Luis I, Irigoyen JJ, Sanchez-Diaz M. 1999. Elevated CO_2 enhances plant growth in droughted N_2-fixing alfalfa without improving water status. *Physiologia Plantarum* **107**: 84–89.

Dickinson RE, Henderson-Sellers A, Kennedy PJ, Wilson MF. 1986. *Biosphere-atmosphere transfer scheme (BATS) for the NCAR community climate model.* Boulder, CO, USA: National Center for Atmospheric Research (NCAR) Technical Note NCAR/TN-275+STR.

Ehrler WJ, Idso SB, Jackson RD, Reginato RJ. 1978. Wheat canopy temperature: relation to plant water potential. *Agronomy Journal of* **70**: 251–256.

Evans JR. 1989. Photosynthesis and nitrogen relationships in leaves of C_3 plants. *Oecologia* **78**: 9–19.

Farquhar GD, Wong SC. 1984. An empirical model of stomatal conductance. *Australian Journal of Plant Physiology* **11**: 191–210.

Farquhar GD, von Caemmerer S. 1982. Modeling of photosynthetic response to environmental conditions. In: Lange OL, Noble PS, Osmond CB, Ziegler H, eds. *Physiological plant ecology II encyclopedia of plant physiology.* Berlin, Germany: Springer-Verlag, 549–587.

Farquhar GD, von Caemmerer S, Berry JA. 1980. A biochemical model of photosynthetic CO_2 assimilation in leaves of C_3-species. *Planta* **149**: 78–90.

Garcia RL, Long SP, Wall GW, Osborne CP, Kimball BA, Nie GY, Pinter Jr PJ, LaMorte RL. 1998. Photosynthesis and conductance of spring wheat leaves: response to free-air atmospheric CO_2 enrichment. *Plant, Cell & Environment* **21**: 659–669.

Genuchten van MTh, Leij FJ, Yates SR. 1992. *The RETC Code for quantifying the hydraulic functions of unsaturated soils.* Ada, USA: EPA report, US Environment Protection Agency, 85 (Assistant Administrator Far Water, Office of Science and Technology).

Gollan T, Schurr U, Schulze ED. 1992. Stomatal responses to drying soil in relation to changes in the xylem sap composition of *Helianthuus Annuus.* I. The concentration of cations, anions, amino acids in, and pH of, the xylem sap. *Plant, Cell & Environment* **15**: 551–560.

Goudriaan J, van Laar HH. 1994. Modeling Crop Growth *Processes current issues in production ecology* 2. Amsterdam, The Netherlands: Kluwer.

Goudriaan J, van Laar HH, van Keulen H, Louwerse W. 1985. Photosynthesis, CO_2 and plant production. In: Day W, Atkin RK, eds. *Wheat growth and modeling. NATO ASI Series. Series A: Life Sciences.* **86**: 107–121.

Grant RF, Wall GW, Kimball BA, Frumau KFA, Pinter Jr PJ, Hunsaker DJ, LaMorte RL. 1999. Crop water relations under different CO_2 and irrigation: testing of *ecosys* with the free air CO_2 enrichment (FACE) experiment. *Agricultural and Forest Meteorology* **95**: 27–51.

Groot JJR. 1987. *Simulation of nitrogen balance in a system of winter wheat and soil.* Wageningen, The Netherlands: Simulation Report, Center of Agrobiological Research (CABO-TT13).

Grossman-Clarke S, Kimball BA, Hunsaker DJ, Long SP, Garcia RL, Kartschall T, Wall GW, Pinter Jr PJ, Wechsung F, LaMorte RL. 1999. Effects of elevated CO_2 on canopy transpiration in senescent spring wheat. *Agricultural and Forest Meteorology* **93**: 95–109.

Hartung W, Slovik S. 1991. Physicochemical properties of plant growth regulators and plant tissues determine their distribution and redistribution: stomatal regulation by abscisic acid in leaves. *New Phytologist* **119**: 361–382.

Hendrey G, Lewin K, Nagy J. 1993. Control of Carbon Dioxide in Unconfined Field Plots. In: Schulze ED, Mooney HA, eds. *Design and Execution of Experiments on CO_2 Enrichment.* Bruessels, Luxembourg: Commission of the European Communities, 309–328.

Hsiao TC, Jackson RB. 1999. Interactive effects of water stress and elevated CO_2 on growth, photosynthesis, and water use efficiency. In: Luo Y, Mooney HA, eds. *Carbon Dioxide and Environmental Stress.* San Diego, CA, USA: Academic Press, 3–31.

Huber SC, Rogers HH, Mowry FL. 1984. Effects of water stress on photosynthesis and carbon partitioning in soybean (*Glycine max.* [L.] Merr.) plants grown in the field at different CO_2 levels. *Plant Physiology* **76**: 244–249.

Hunsaker DJ, Kimball BA, Pinter Jr PJ, LaMorte RL, Wall GW. 1996. Effects of CO_2 enrichment and irrigation on soil water balance evapotranspiration of wheat grown under open-air field conditions. *Transactions of the ASAE* **4**: 1345–1355.

Idso SB, Reginato RJ, Reicosky DC, Hatfield JL. 1981. Determining soil-induced plant water potential depressions in alfalfa by means of infrared thermometry. *Agronomy Journal of* **73**: 826–830.

Idso SB, Jackson RD. 1969. Thermal radiation from the atmosphere. *Journal of Geophysical Research* **74**: 5397–5403.

Jackson RD, Idso SB, Reginato RJ, Pinter Jr PJ. 1981. Canopy temperature as a crop water stress indicator. *Water Resources Research* **17**: 1133–1138.

Jacobs CMJ, van den Hurk BJJM, de Bruin HAR. 1996. Stomatal behavior and photosynthetic rate of unstressed grapevines in semi-arid conditions. *Agricultural and Forest Meteorology* **80**: 111–134.

Kartschall Th, Grossman S, Wechsung F, Gräfe J, Poschenrieder W. 1996. *Untersuchung der Auswirkungen Von Klimaänderungen Auf Agrarökosysteme. Abschlußbericht zum BMBF-Vorhaben 01LK9107–5.* Potsdam, Germany: Potsdam-Institut für Klimafolgenforschung e. V.

Kartschall Th, Döring P, Suckow F. 1989. Simulation of Nitrogen, water and temperature dynamics in soil. *Systems Analysis, Modelling and Simulation* **6**: 117–123.

van Keulen H, Seligman NG. 1987. *Simulation of water use, nitrogen nutrition and growth of a spring wheat crop* Wageningen, The Netherlands: Centre for Agricultural Publishing and Documentation (Pudoc).

Kimball BA, LaMorte RL, Pinter PJ, JrWall GW, Hunsaker DJ, Adamsen FJ. 1999. Free-air CO_2 enrichment (FACE) and soil nitrogen effects on energy balance and evapotranspiration of wheat. *Water Resources Research* **35**: 1179–1190.

Kimball BA, Pinter Jr PJ, Garcia RL, LaMorte RL, Wall GW, Hunsaker DJ, Wechsung G, Wechsung F, Kartschall T. 1995. Productivity and water use of wheat under free-air CO_2 enrichment. *Global Change Biology* **1**: 429–442.

Kimball BA, LaMorte RL, Seay RS, Pinter PJ, JrRockey RR, Hunsaker DJ, Dugas WA, Heuer ML, Mauney JR, Hendrey GR, Lewin KF, Nagy J. 1994. Effects of free-air CO_2 enrichment on energy balance and evapotranspiration of cotton. *Agricultural and Forest Meteorology* **70**: 259–278.

Kimball BA, La Morte RL, Peresta GJ, Mauney JR, Lewin KF, Hendrey GR. 1993. Appendices I, II-A, II-B, II-C, II-D. In: Hendrey GR, ed. *FACE: Free-Air Carbon Dioxide Enrichment for Plant Research in the Field.* Bota Racon, FL, USA: CRC Press, 271–308.

Kimball BA. 1983. Carbon dioxide and agricultural yield: an assemblage and analysis of 430 prior observations. *Journal of Agronomy* **75**: 779–788.

Kimball BA, Idso SB. 1983. Increasing atmospheric CO_2: effects on crop yield, water use and climate. *Agric Water Management* **7**: 55–73.

Leuning R, Dunin FX, Wang YP. 1998. A two-leaf model for canopy conductance, photosynthesis and partitioning of available energy. II. Comparison with measurements. *Agricultural and Forest Meteorology* **91**: 113–125.

Long SP. 1991. Modification of the response of photosynthetic productivity to rising temperature by atmospheric CO_2 concentrations: Has its importance been underestimated? *Plant, Cell & Environment* **14**: 729–739.

Mahrt L, Ek M. 1984. The influence of atmospheric stability on potential evaporation. *Journal of Climate and Applied Meteorology* **23**: 222–234.

Morison JIL. 1998. Stomatal response to increased CO_2 concentration. *Journal of Experimental Botany* **49**: 443–452.

Mualem Y. 1976. A new model for predicting the hydraulic conductivity of unsaturated porous media. *Water Resources Research* **12**: 513–522.

Osborne CP, LaRoche J, Garcia RL, Kimball BA, Wall GW, Pinter PJ Jr, LaMorte RL, Hendrey GR, Long SP. 1998. Does leaf position within a canopy affect acclimation of photosynthesis to elevated CO_2? Analysis of a wheat crop under Free-Air CO_2 enrichment. *Plant Physiology* **117**: 1037–1045.

Penning de Vries FWT, Jansen DM, ten Berge HFM, Bakema A. 1989. *Simulation of ecophysiological processes of growth in several annual crops.* Wageningen, The Netherlands: Centre for Agricultural Publishing and Documentation (Pudoc).

Penning de Vries FWT, van Laar HH. 1982. *Crop Production* Wageningen, The Netherlands: Centre for Agricultural Publishing and Documentation (Pudoc).

Pinter PJ, JrKimball BA, Wall GW, LaMorte RL, Hunsaker DJ, Adamsen FJ, Frumau KFA, Vugts HF, Hendrey GR, Lewin KF, Nagy J, Johnson HB, Wechsung F, Leavitt SW, Thompson TL, Matthias AD, Brooks TJ. 2000. Free-air CO_2 enrichment (FACE): blower effects on wheat canopy microclimate and plant development. *Agricultural and Forest Meteorology* **103**: 319–333.

Pinter Jr PJ, Kimball BA, Garcia RL, Wall GW, Hunsaker DJ, LaMorte RL. 1996. Free-air CO_2 enrichment: responses of cotton and wheat crops. In: Koch GW, Mooney HA, eds. *Carbon Dioxide and terrestrial ecosystems* San Diego, CA, USA: Academic Press, 215–264.

Pinter Jr PJ, Reginato RJ. 1982. A thermal infrared technique for monitoring cotton water stress and scheduling irrigations. *Transactions of the ASAE* **25**: 1651–1655.

de Pury DGG, Farquhar GD. 1997. Simple scaling of photosynthesis from leaves to canopies without the errors of big-leaf models. *Plant, Cell & Environment* **20**: 537–557.

Raschke K. 1987. Action of abscisic acid on guard cells. In: Zeiger E, Farquhar GD, Cowan IR, eds. *Stomatal function.* Stanford, CA, USA: Stanford University Press, 253–279.

Raupach MR, Finnigan JJ. 1988. 'Single-layer models of evaporation from plant canopies are incorrect but useful, whereas multilayer models are correct but useless': discuss. *Australian Journal of Plant Physiology* **15**: 705–716.

Schulze ED, Turner NC, Gollan T, Shackel KA. 1987. Stomatal responses to air humidity and soil drought. In: Zeiger E, Farquhar GD, Cowan IR, eds. *Stomatal function.* Stanford, CA, USA: Stanford University Press, 311–321.

Seligman NG, Loomis RS, Burke J, Abshahi A. 1983. Nitrogen nutrition and phenological development in field-grown wheat. *Journal of Agricultural Science* **101**: 691–697.

Shuttleworth WJ. 1991. Evaporation models in hydrology. In: Schmugge TJ, Andre JC, eds. *Measurement and parameterization of land surface evaporation fluxes* New York, USA: Springer Verlag, 93–120.

Stitt M. 1991. Rising CO_2 levels and their potential significance for carbon flow in photosynthetic cells. *Plant, Cell & Environment* **14**: 741–762.

Stockle CO. 1991. Canopy photosynthesis and transpiration estimates using radiation interception models with different levels of detail. *Ecological Modelling* **60**: 31–44.

Tardieu F, Simonneau T. 1998. Variability among species of stomatal control under fluctuating soil water status and evaporative demand: modeling isohydric and anisohydric behaviors. *Journal of Experimental Botany* **49**: 419–432.

Tenhunen JD, Pearcy RW, Lange OL. 1987. Diurnal variations in leaf conductance and gas exchange in natural environments. In: Zeiger E, Farquhar GD, Cowan IR, eds. *Stomatal function.* Stanford, CA, USA: Stanford University Press, 323–351.

Therashima I. 1992. Anatomy of nonuniform leaf photosynthesis. *Photosynthesis Research* **31**: 195–212.

Tubiello FN, Rosenzweig C, Kimball BA, Pinter Jr PJ, Wall GW, Hunsaker DJ, LaMorte RL, Garcia RC. 1999. Testing CERES-wheat with free-air carbon dioxide enrichment (FACE) experiment data: CO_2 and water interactions. *Agronomy Journal of* **91**: 247–255.

von Caemmerer S, Evans JR, Hudson GS, Andrews TJ. 1994. The kinetics of ribulose-1,5-bisphosphate carboxylase/oxygenase in vivo inferred from measurements of photosynthesis in leaves of transgenic tobacco. *Planta* **195**: 88–97.

Wang YP, Leuning R. 1998. A two-leaf model for canopy conductance, photosynthesis and partitioning of available energy I: Model description and comparison with a multi layered model. *Agricultural and Forest Meteorology* **91**: 89–111.

Wechsung G, Wechsung F, Wall GW, Adamsen FJ, Kimball BA, Pinter Jr PJ, Lamorte RL, Garcia RL, Kartschall T. 1999. The effects of free-air CO_2 enrichment and soil water availability on spatial and seasonal patterns of wheat root growth. *Global Change Biology* **5**: 519–530.

Zadoks JC, Chang TT, Konzak CF. 1974. A decimal code for the growth stages of cereals. *Wheat Research* **14**: 415–421.

Appendix 1

Energy fluxes between soil, canopy and atmosphere

$$\lambda E_c = \frac{\rho_a c_p V_m[e_s(T_c) - e_a]}{\gamma[(g_{s,c} + 1.6 LAI \cdot g_c)^{-1} + 0.93\, g_{b,h}^{-1}]} \qquad \text{Eqn A1}$$

$$\lambda E_s = \frac{\rho_a c_p V_m[e_s(T_s) - e_a]}{\gamma(g_{s,s}^{-1} + 0.93 \cdot g_{b,s}^{-1})} \qquad \text{Eqn A2}$$

$$H_c = \rho_a c_p V_m g_{b,h}(T_c - T_a) \qquad \text{Eqn A3}$$

$$H_s = \rho_a c_p V_m g_{b,s}(T_s - T_a) \qquad \text{Eqn A4}$$

Equation to determine vapor pressure (e_a) and air temperature (T_a) inside the canopy:

$$E_c + E_s = \frac{\rho_a c_p(e_a - e_r)}{\gamma \lambda r_a} \qquad \text{Eqn A5}$$

$$H_c + H_s = \frac{\rho_a c_p(T_a - T_r)}{r_a} \qquad \text{Eqn A6}$$

$$g_{b,h} = \frac{LAI u_a^{0.5}}{180\, w_l^{0.5} V_m} \qquad g_{b,s} = \frac{u_a^{0.5}}{180\, w_s^{0.5} V_m} \qquad \text{Eqn A7}$$

$$u_a = \frac{u^*}{k}\ln\left[\frac{(h_c - d)}{z_0}\right]\exp(-2L) \qquad u^* = \frac{k u_r}{\ln[(z_r - d) \cdot z_0^{-1}]} \qquad \text{Eqn A8}$$

$$r_a = \frac{\{\ln[(z_r - d + z_0) z_0^{-1}]\}^2}{k^2 u_r}\, \Psi \qquad \text{Eqn A9}$$

$$\Psi = \begin{cases} 1.0 & neutral \\ (1 + 15 Ri)(1 + 5 Ri)^{0.5} & stable \\ \{1 - 15 Ri[1 + K(-Ri)^{0.5}]^{-1}\}^{-1} & unstable \end{cases} \qquad \text{Eqn A10}$$

$$Ri = \frac{g(T_r - T_a)(z_r - d)}{u_r^2 T_r}$$

$$K = \frac{75 k^2[(z_r - d + z_0) z_0^{-1}]^{0.5}}{\{\ln[(z_r - d + z_0) z_0^{-1}]\}^2} \qquad \text{Eqn A11}$$

Canopy net assimilation rate and canopy conductance

$$A_{n,c} = \int_0^{LAI} A_n(L)dL \approx \sum_{i=1}^{p} A_n(L_i)\Delta L_i \qquad \text{Eqn A12}$$

$$g_{s,c} = \int_0^{LAI} g_s(L)dL \approx \sum_{i=1}^{p} g_s(L_i)\Delta L_i = \frac{1.6 A_{n,c}}{C_s - C_i} \qquad \text{Eqn A13}$$

Net leaf assimilation rate

$$A_n = \left(1 - \frac{\Gamma_*}{c_c}\right)\min\{W_j, W_c\} - R_d \qquad \text{Eqn A14}$$

$$\Gamma_* = \frac{0.5 V_{o\max} K_c o_i}{V_{c\max} K_o} \qquad \text{Eqn A15}$$

$$V_{c\max} = 1.25 k_{cat} f_{Rub} N_l \qquad V_{o\max} = 0.21 V_{c\max} \qquad \text{Eqn A16}$$

$$W_c = V_{c\max}\frac{c_c}{c_c + K_c(1 + o_i/K_o)} \qquad W_j = \frac{c_c J_e}{4 c_c + 8\Gamma_*} \qquad \text{Eqn A17}$$

$$\Omega_J J_e^2 - (I_{eff} + J_{max})J_e + I_{eff} J_{max} = 0$$
$$I_{eff} = 0.5 I_{abs}(1 - f_c) \qquad \text{Eqn A18}$$

$$J_{max} = 2.1 V_{c\max} \quad \text{at } 25°C \qquad \text{Eqn A19}$$

$$V_{c\max}(T) = V_{c\max}(T_0)\exp\left[\frac{(T - T_0)E_A}{T_0 R \cdot T}\right]\left(\frac{T}{T_0}\right)^{0.5} \qquad \text{Eqn A20}$$

$$J_{max}(T) = J_{max}(T_0)\frac{\exp[(-E_A/RT_0)(1 - T_0/T)]}{1 + \exp[(S_A T_c - H_A)/(RT)]} \qquad \text{Eqn A21}$$

$$c_c = c_i - \frac{A_{n,c}}{g_m LAI} \qquad \text{Eqn A22}$$

$$g_m = \frac{V_{c\max}}{200 + V_{c\max}} \qquad \text{Eqn A23}$$

$$c_s = c_r - A_{n,c}\left(\frac{1.32}{g_{b,h}} + 1.4 r_a V_m\right) \qquad \text{Eqn A24}$$

Leaf internal CO_2 concentration (c_i)

$$f = \frac{c_i - \Gamma}{c_s - \Gamma} = f_{max}\left(1 - \frac{D_s}{D_{max}}\right) + f_{min}\frac{D_s}{D_{max}} \qquad \text{Eqn A25}$$

$$\Gamma = \frac{\Gamma_* + K_c(1 + o_i/K_o)R_d/V_{c\max}}{1 - R_d/V_{c\max}} \qquad \text{Eqn A26}$$

$$f_{min} = \frac{g_c}{g_c + g_m} \qquad \text{Eqn A27}$$

$$f_{max} = \frac{f_0 - f_{min} D_0 D_{max}^{-1}}{1 - D_0 D_{max}^{-1}} \qquad \text{Eqn A28}$$

Energy balance equation of the canopy for determining canopy temperature (T_c):

$$F(T_c) = R_{n,c}(T_c) - H_c(T_c) - \lambda E_c(T_c) - c_l\frac{dT_c}{dt} - \qquad \text{Eqn A29}$$
$$\lambda E_p(T_c) - P_i c_w(T_c - T_a) = 0$$

$$T_c^{n+1} = \frac{T_c^n F'(T_c^n) - F(T_c^n)}{F'(T_c^n)} \qquad \text{with}$$

Eqn A30

$$F'(T_c^n) = \frac{\delta F(T_c^n)}{\delta T_c^n}$$

Equation for determining the CO_2 concentration in the chloroplasts (c_c):

$$F(c_c) = c_r - c_c - A_{n,c}(c_c)\left(1.4 r_a V_m + \frac{1.32}{g_{b,h}} + \frac{1.6}{g_{s,c} + 1.6 g_c LAI} + \frac{1}{g_m LAI}\right) = 0$$

Eqn A31

$$c_c^{n+1} = \frac{c_c^n F'(c_c^n) - F(c_c^n)}{F'(c_c^n)} \qquad \text{with}$$

Eqn A32

$$F'(c_c^n) = \frac{\delta F(c_c^n)}{\delta c_c^n}$$

New
Phytologist

Appendix 2

Definition of symbols

Term	Units	Definition
A_n	$\mu mol\ m^{-2}\ s^{-1}$	Net leaf rate of CO_2 uptake per unit leaf area
$A_{n,c}$	$\mu mol\ m^{-2}\ s^{-1}$	Net canopy rate of CO_2 uptake per unit ground area
c_c	$\mu mol\ mol^{-1}$	CO_2 concentration in the chloroplasts
c_i	$\mu mol\ mol^{-1}$	Intercellular CO_2 concentration in air
c_l	$J\ K^{-1}$	Heat capacity of green biomass: with m_{gbm} above-ground dry biomass, c_{gbm} specific heat capacity of dry biomass ($2.5 \cdot 10^6\ J\ kg^{-1}\ K^{-1}$).
c_p	$J\ kg^{-1}\ K^{-1}$	Specific heat capacity of air at constant pressure (1005)
c_w	$J\ kg^{-1}\ K^{-1}$	Specific heat capacity of water ($4.187 \cdot 10^6$)
c_r	$\mu mol\ mol^{-1}$	CO_2 concentration at reference height
c_s	$\mu mol\ mol^{-1}$	CO_2 concentration at the 'big leaf' surface
d	m	Zero plane displacement ($d = 0.63 h_c$)
D_0	$g\ kg^{-1}$	Stomata are not influenced by D_s for $D_s < D_0$ (cp. paragraph 2.3)
D_{max}	$g\ kg^{-1}$	Value of D_s where stomata close completely (cp. paragraph 2.3)
D_s	$g\ kg^{-1}$	Specific humidity deficit at the 'big leaf' surface
e_a	Pa	Vapor pressure inside the canopy
e_r	Pa	Vapor pressure at reference height
e_s	Pa	Saturation vapor pressure at T_c or T_s
E_A	$J\ mol^{-1}$	Activation energy for the kinetic constants of Rubisco, K_c (65 800), K_o (1400), V_{cmax} (68 000), J_{max} (37 000)
E_c	$kg\ m^{-2}\ s^{-1}$	Canopy transpiration rate per unit ground area
E_p	$kg\ m^{-2}\ s^{-1}$	Potential rate of canopy transpiration per unit ground area
E_r	$kg\ m^{-2}\ s^{-1}$	Evaporation rate of intercepted rain and dew per unit ground area
E_s	$kg\ m^{-2}\ s^{-1}$	Soil evaporation rate per unit ground area
f	–	$(c_i - \Gamma)/(c_s - \Gamma)$
f_c	–	Spectral correction factor (0.15)
f_{max}	–	f at $D_s = 0$
f_{min}	–	f at $D_s = D_{max}$
f_{rub}	–	Fraction of N_l contained in Rubisco (0.23)
f_0	–	f at $D_s < D_0$ (0.7)
g	$m\ s^{-2}$	Gravity constant (9.81)
$g_{b,h}$	$mol\ m^{-2}\ s^{-1}$	Canopy boundary layer conductance for heat per unit ground area
$g_{b,s}$	$mol\ m^{-2}\ s^{-1}$	Soil boundary layer conductance for heat per unit ground area
g_c	$mol\ m^{-2}\ s^{-1}$	Leaf cuticular conductance for CO_2 per unit leaf area (0.01)
g_m	$mol\ m^{-2}\ s^{-1}$	Leaf mesophyll conductance for CO_2 per unit leaf area
g_s	$mol\ m^{-2}\ s^{-1}$	Leaf stomatal conductance for H_2O per unit leaf area
$g_{s,c}$	$mol\ m^{-2}\ s^{-1}$	Canopy conductance for H_2O per unit ground area
$g_{s,s}$	$mol\ m^{-2}\ s^{-1}$	Soil surface conductance for H_2O per unit ground area
h_c	m	Canopy height
H_A	$J\ mol^{-1}$	Constant for determining the temperature dependence of J_{max} (220 000)
H_c	Wm^{-2}	Canopy sensible heat flux per unit ground area
H_s	Wm^{-2}	Soil sensible heat flux per unit ground area
I_{abs}	$\mu mol\ m^{-2}\ s^{-1}$	Absorbed photon flux per unit leaf area
I_{eff}	$\mu mol\ m^{-2}\ s^{-1}$	Effectively absorbed PAR by photosystem II per unit leaf area
I_s	–	Crop Water Stress Index
J_e	$\mu mol\ m^{-2}\ s^{-1}$	Rate of electron transport per unit leaf area
J_{max}	$\mu mol\ m^{-2}\ s^{-1}$	Potential rate of electron transport per unit leaf area
k	–	von Karman constant (0.41)
k_{cat}	$mol\ mol^{-1}\ s^{-1}$	Catalytic constant for RuP_2 carboxylation (3.3)
K_c	$\mu mol\ mol^{-1}$	Michaelis–Menten constant for CO_2 (259)
K_o	$mmol\ mol^{-1}$	Michaelis–Menten constant for O_2 (179)
L	$m^2\ m^{-2}$	Depth inside the canopy with respect to leaf area
L_i	$m^2\ m^{-2}$	Depth of ith-layer inside the canopy
LAI	$m^2\ m^{-2}$	Leaf area index
n	–	Number of the iteration step at time t
N_l	$mmol\ m^{-2}$	Leaf nitrogen content per unit leaf area
o_i	$mmol\ mol^{-1}$	Intercellular concentration of O_2 in air (210)
p	–	Number of canopy layers for the calculation of $A_{n,c}$ and $g_{s,c}$ ($p \leq 20$)
P_i	$kg\ m^{-2}\ s^{-1}$	Intercepted rain and dew per unit ground area

Appendix 2 *continued*

Term	Units	Definition
r_a	s m^{-1}	Aerodynamic resistance
R	Pa m^3 mol^{-1} K^{-1}	Molar gas constant (8.314)
R_d	µmol m^{-2} s^{-1}	Dark respiration per unit leaf area
$R_{n,c}$	Wm^{-2}	Net radiation balance of the canopy
Ri	–	Richardson number
S_A	J K^{-1} mol^{-1}	Constant for determining the temperature dependence of J_{max} (710)
t	s	Time
T	K	Temperature
T_0	K	Basis temperature for kinetic constants of Rubisco (298 K)
T_a	K	Air temperature inside the canopy
T_c	K	Canopy temperature
T_r	K	Air temperature at reference height
T_s	K	Soil surface temperature
u_a	m s^{-1}	Wind speed inside the canopy
u_r	m s^{-1}	Wind speed at reference height
$u*$	m s^{-1}	Friction velocity
$V_{c\,max}$	µmol m^{-2} s^{-1}	Maximum capacity of RuP$_2$ carboxylation per unit leaf area ( )
$V_{o\,max}$	µmol m^{-2} s^{-1}	Maximum capacity of RuP$_2$ oxygenation per unit leaf area
V_m	m^3 mol^{-1}	Molar volume of the air ($V_m = RT_a/p_a$, with p_a air pressure)
w_l	m	Leaf width (0.01)
w_s	m	Size of soil particles (0.005)
W_c	µmol m^{-2} s^{-1}	RuP$_2$-saturated rate of CO$_2$ assimilation per unit leaf area
W_j	µmol m^{-2} s^{-1}	RuP$_2$-limited rate of CO$_2$ assimilation per unit leaf area
z_0	m	Roughness length ($z_0 = 0.13h_c$)
z_r	m	Reference height in the atmosphere (2m)
ΔL_i	m^2 m^{-2}	Width with respect to leaf area index of the ith-canopy layer
γ	Pa K^{-1}	Psychrometric constant ($V_m = RT_a/p_a$, with pa air pressure)
Γ	µmol mol^{-1}	CO$_2$ compensation point of photosynthesis
$\Gamma*$	µmol mol^{-1}	CO$_2$ compensation point of photosynthesis in the absence of R_d
λ	J kg^{-1}	Latent heat of vaporization (2.45 × 10^6)
λE_c	W m^{-2}	Canopy latent heat flux according to transpiration
λE_p	W m^{-2}	Latent heat flux according to evaporation of P_i
λE_s	W m^{-2}	Soil latent heat flux
Ω_j	–	Parameter to describe convexity of J_e with respect to I_{eff} (0.7)
Ψ	–	Stability function of aerodynamic resistance
ρ_a	kg m^{-3}	Air density